Int J Adv Eng Sci Appl Math (2009) 1:1–24

IIT, Madras

ORIGINAL PAPER

Challenges of porous media models in geo- and biomechanical engineering including electro-chemically active polymers and gels

Wolfgang Ehlers

© Indian Institute of Technology, Madras

Abstract Miscible multi-component materials like classical mixtures as well as immiscible materials like saturated and partially saturated porous media can be successfully described on the common basis of the well-founded Theory of Mixtures (TM) or the Theory of Porous Media (TPM). In particular, both the TM and the TPM provide an excellent framework for a macroscopic description of a broad variety of applications ranging, for example, from standard and sophisticated problems in geomechanics via biomechanical applications to electro-chemically active polymers and gels, etc. The present article portrays general multiphasic and multi-component materials, thus reflecting their mechanical and their thermodynamical framework, while furthermore adding electro-chemical effects. Including some constitutive models and illustrative numerical examples, the article can be understood as a reference to theoretical and numerical investigations in the broad field of porous media models.

Keywords Theory of porous media · Solid-fluid interaction · Electro-chemical effects · Finite solid elasticity · Solid elasto-plasticity · Fluid transport · Ion diffusion · Finite element analysis

1 Introduction

In many branches of engineering as well as in applied natural sciences, one often has to deal with continuum-mechanical and structural problems which cannot be uniquely classified within the well-known disciplines of either "solid mechanics" or "fluid mechanics". These problems, characterised by the fact that they require a unified treatment of volumetrically coupled solid-fluid aggregates, basically fall into the categories of porous media models. Following this, there is a broad variety of applications ranging in this category as for example the analysis of coupled solid deformation and pore-fluid flow behaviour of saturated or partially saturated soil, the investigation of foamed metals and polymers under consideration of their pore content, the description of biological soft and hard tissue or the study of electro-chemically active polymers and gels.

Analysing porous media models on a continuum-mechanical basis implies the investigation of an immiscible aggregate of a solid skeleton and a pore-fluid content, which can either be a single liquid or a single gas or a combination of liquids and gases, which itself might be chemically miscible or immiscible. If real mixtures are concerned, one directly proceeds from the assumption of a continuum with statistically distributed components being completely smeared out through the considered domain in the sense of superimposed and interacting continua. Proceeding from this image directly leads to the basic assumptions of the classical Theory of Mixtures (TM) assuming heterogeneously composed continua consisting of an arbitrary number of miscible and interacting constituents. Concerning the evolution of the TM, the reader is referred to the work by Truesdell [54], Truesdell and Toupin [56], Bowen [9] or the later work by Truesdell [55] and the quotations therein.

Regarding the Theory of Mixtures, there is no measure to incorporate any kind of micro-structural information. As a result, it was found convenient to combine the "Theory of Mixtures" with the "Concept of Volume Fractions" in order to describe structured materials like porous solids. By use of this procedure, basically defining the "Theory of Porous Media" (TPM), cf. e.g. the work by Bowen [10, 11], de Boer [3, 4], de Boer and Ehlers [5–7] or Ehlers [14–16, 18, 19], one obtains an excellent tool for the macroscopic description of general immiscible multiphasic aggregates, where the volume fractions are the measures of the local portions of the individual constituents of the overall medium and where

Wolfgang Ehlers
Fakultat Bau-und mweltingenieurwissenschaften Institut fur Mechanik (Bauwesen), Lehrustuhl II Universitat Stuttgart, Pfaffenwaldring 7, 70569 Stuttgart, Germany
E-mail: ehlers@mechbau.uni-stuttgart.de

all incorporated fields are understood as local averages of the corresponding quantities of the underlying micro-structure.

It is the goal of the present contribution to exhibit the fundamental concepts of the Theory of Porous Media, and to present some illustrative applications exhibiting the high level of sophistication of this approach. In this regard, two basically different models are discussed. These are, firstly, an unsaturated soil investigated as a triphasic, three-component material of a solid skeleton and an immiscible pore content of water and air. Apart of the general discussion of this model in the framework of small-strain elasto-plasticity, numerical examples show the flow of water through a deformable embankment of a river at different water levels, where, as a result of the technical layout of the dam, not only stable but also unstable situations are presented. Secondly, a swelling medium is considered consisting of a swellable solid skeleton and a miscible pore content of a liquid solvent and dissolved solutes. In addition, electro-chemical reactions can be taken into account. Since swelling media can undergo large deformations, this model is treated in the framework of finite-strain elasticity. Based on this procedure, not only swelling media such as active soil or soft biological tissue can be described but also electro-active polymers and gels, where the application of an electrical potential leads to local deformations of the charged aggregate.

2 Preliminaries

2.1 Immiscible components and volume fractions

In case of immiscible components constituting the overall aggregate, the TPM provides the volume fractions as a measure of the local portions of the individual materials, such as the solid skeleton and the pore fluids, liquids and gases. The introduction of volume fractions as one of the fundamental concepts of the TPM proceeds from the assumption of a statistical distribution of the individual constituents over the control space. This assumption together with the prescription of a real or a virtual averaging process leads to a model φ of superimposed and interacting continua φ^α ($\alpha = 1, \dots, k$):

$$\varphi = \bigcup_{\alpha=1}^{k} \varphi^\alpha \,. \tag{1}$$

Thus, each spatial point $\mathbf{x}$ of the control space Ω is simultaneously occupied by particles P^α of all k constituents. Consequently, the mathematical functions for the description of the geometrical and physical properties of the individual materials are field functions defined in the complete control space. The volume V of the overall multiphasic and multicomponent aggregate $\mathscr{B}$ results from the sum of the partial volumes of the constituents φ^α in $\mathscr{B}$:

$$V = \int_{\mathscr{B}} \mathrm{d}v = \bigcup_{\alpha=1}^{k} V^\alpha \,,$$

where

$$V^\alpha = \int_{\mathscr{B}} \mathrm{d}v^\alpha =: \int_{\mathscr{B}} n^\alpha \, \mathrm{d}v \,. \tag{2}$$

Following this, the quantity n^α is defined as the local ratio of the volume element $\mathrm{d}v^\alpha$ of a given constituent φ^α with respect to the volume element $\mathrm{d}v$ of the overall medium φ:

$$n^\alpha = \frac{\mathrm{d}v^\alpha}{\mathrm{d}v} \,. \tag{3}$$

The relations (2) and (3) represent the concept of volume fractions. Since, in general, there is no vacant space in the overall medium, equation (2) directly leads to the saturation condition

$$\sum_{\alpha=1}^{k} n^\alpha = 1 \,. \tag{4}$$

By use of the volume fractions n^α, two different density functions can be introduced:

$$\rho^{\alpha R} = \frac{\mathrm{d}m^\alpha}{\mathrm{d}v^\alpha} \quad \text{and} \quad \rho^\alpha = \frac{\mathrm{d}m^\alpha}{\mathrm{d}v} \,. \tag{5}$$

The effective density $\rho^{\alpha R}$ represents the local average of the real material density of φ^α by relating the local mass $\mathrm{d}m^\alpha$ to the volume element $\mathrm{d}v^\alpha$, whereas the partial density ρ^α relates the same mass to the bulk volume element $\mathrm{d}v$. Following this, the density functions are coupled by the volume fractions:

$$\mathrm{d}m^\alpha = \left\{ \begin{matrix} \rho^{\alpha R} \, \mathrm{d}v^\alpha \\ \rho^\alpha \, \mathrm{d}v \end{matrix} \right\} \longrightarrow \rho^\alpha = n^\alpha \, \rho^{\alpha R} \,. \tag{6}$$

Based on the above relation, it is immediately evident that the property of material incompressibility ($\rho^{\alpha R} = \text{const.}$) is not equivalent to the property of bulk incompressibility of this constituent, since the partial density functions ρ^α can still change through changes in the volume fractions n^α.

In addition to the volume fractions, it is convenient for several applications to introduce the so-called saturation functions s^β defined as the volume fractions of the pore fluids with respect to the pore space. Thus, in case of l pore fluids ($l = k - 1$), one obtains

$$s^\beta = \frac{n^\beta}{n^F}, \quad \text{where} \quad n^F = \sum_{\beta=1}^{l} n^\beta \quad \text{and} \quad \sum_{\alpha=1}^{l} s^\beta = 1 \,. \tag{7}$$

Therein, n^F is the volume fraction of the accumulated pore fluids or the porosity, respectively.

2.2 Miscible components and molar concentrations

Assume that the pore space is saturated by a real fluid mixture or by a solution of a solute and dissolved solvents. In this case, it is necessary to distinguish differently between the components compared to the introduction of volume fractions. Proceeding from the fact that volume fractions cannot be measured in case of real mixtures, the mixture components are considered by their partial densities ρ_F^β defined with respect to the pore space (pore densities). Thus,

$$\rho^\beta =: n^F \rho_F^\beta, \quad \text{where} \quad \rho^{FR} = \sum_{\beta=1}^{l} \rho_F^\beta \quad \text{and}$$

$$\rho^F = n^F \rho^{FR}. \tag{8}$$

Comparable to the Theory of Mixtures, ρ^{FR} here defines the so-called mixture density of the pore content (pore mixture density) given through the sum of the partial pore densities. Furthermore, ρ^F relates ρ^{FR} to the volume of the whole aggregate, while ρ^{FR} itself is related to the pore space.

Given ρ_F^β, the portion of matter is defined through the molar concentration c_m^β and the molar mass M_m^β via

$$\rho_F^\beta = c_m^\beta M_m^\beta, \quad \text{where} \quad c_m^\beta = \frac{\mathrm{d}n_m^\beta}{\mathrm{d}v^F}. \tag{9}$$

Therein, $\mathrm{d}n_m^\beta$ is the local number of moles. Since M_m^β is a constant of the species φ^β, the variation of ρ_F^β is uniquely determined by c_m^β.

3 Kinematical relations

Proceeding from the basic concepts of the Theory of Porous Media, cf. e.g. Ehlers [19], one directly applies the concept of superimposed continua with internal interactions and individual states of motion. In the framework of this concept, each spatial point $\mathbf{x}$ of the current configuration is simultaneously occupied by material particles (material points) P^α of all constituents φ^α ($\alpha = S$: solid skeleton, $\alpha = \beta$: l pore fluids). These particles proceed from different reference positions at time t_0, cf. Figure 1. Thus, each constituent is assigned its own motion function

$$\mathbf{x} = \chi_\alpha(\mathbf{X}_\alpha, t). \tag{10}$$

As a result of the image of superimposed continua, each spatial point $\mathbf{x}$ can only be occupied by one single material point P^α of each constituent φ^α. The assumption of unique motion functions, where each material point P^α of the current configuration has a unique reference position $\mathbf{X}_\alpha$ at time t_0, furthermore requires the existence of unique inverse motion functions χ_α^{-1} based on non-singular Jacobian determinants J_α:

$$\mathbf{X}_\alpha = \chi_\alpha^{-1}(\mathbf{x}, t), \quad J_\alpha = \det \frac{\partial \chi_\alpha}{\partial \mathbf{X}_\alpha} \neq 0. \tag{11}$$

It follows from (10) that each constituent has its own velocity and acceleration fields. In the basic Lagrangean setting, these fields are given by

$$\mathbf{x}'_\alpha = \frac{\partial \chi_\alpha(\mathbf{X}_\alpha, t)}{\partial t}, \quad \mathbf{x}''_\alpha = \frac{\partial^2 \chi_\alpha(\mathbf{X}_\alpha, t)}{\partial t^2}. \tag{12}$$

With the aid of the inverse motion function $(11)_1$, an alternative formulation of (12) leads to the Eulerian description

$$\mathbf{x}'_\alpha = \mathbf{x}'_\alpha(\mathbf{x}, t), \quad \mathbf{x}''_\alpha = \mathbf{x}''_\alpha(\mathbf{x}, t). \tag{13}$$

Suppose that Γ is an arbitrary, steady and sufficiently often steadily differentiable scalar function of $(\mathbf{x}, t)$, then, the material time derivative of Γ following the motion of φ^α reads

$$(\Gamma)'_\alpha = \frac{\mathrm{d}_\alpha}{\mathrm{d}t}\Gamma = \frac{\partial \Gamma}{\partial t} + \operatorname{grad}\Gamma \cdot \mathbf{x}'_\alpha, \tag{14}$$

where the operator "grad $(\cdot)$" denotes the partial derivative of $(\cdot)$ with respect to the local position $\mathbf{x}$.

Describing coupled solid-fluid problems, it is generally convenient to proceed from a Lagrangean description of the solid matrix φ^S using the solid displacement vector $\mathbf{u}_S$ as the

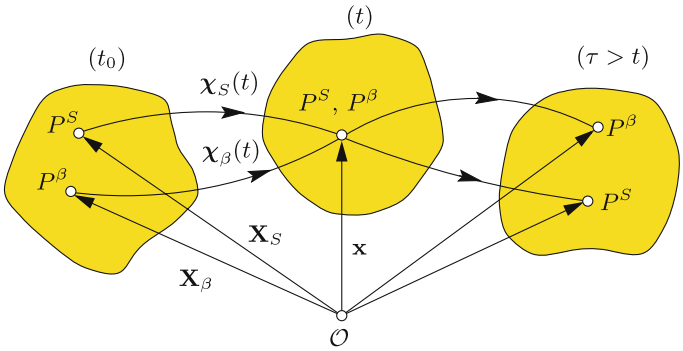

Fig. 1. Motion of a superimposed multi-component aggregate.

primary kinematic variable, whereas the l pore fluids φ^β are better described in a modified Eulerian setting by use of the seepage velocities $\mathbf{w}_\beta$ describing the fluid motions with respect to the deforming skeleton material:

$$\mathbf{u}_S = \mathbf{x} - \mathbf{X}_S, \;\; \mathbf{w}_\beta = \mathbf{x}'_\beta - \mathbf{x}'_S \;\; \text{and} \;\; \mathbf{x}'_S = (\mathbf{u}_S)'_S. \tag{15}$$

In case of a pore-fluid mixture, the barycentric fluid velocity or the pore mixture velocity, respectively, and the corresponding pore diffusion velocity are given by

$$\mathbf{x}'_F = \frac{1}{\rho^{FR}} \sum_{\beta=1}^{l} \rho_F^\beta \mathbf{x}'_\beta \quad \text{and} \quad \mathbf{d}_{\beta F} = \mathbf{x}'_\beta - \mathbf{x}'_F. \tag{16}$$

From (10) and $(11)_1$, one obtains the general material deformation gradient $\mathbf{F}_\alpha$ and its inverse $\mathbf{F}_\alpha^{-1}$ by

$$\mathbf{F}_\alpha = \mathrm{Grad}_\alpha \mathbf{x}, \quad \mathbf{F}_\alpha^{-1} = \mathrm{grad}\, \mathbf{X}_\alpha. \tag{17}$$

Therein, the operator "$\mathrm{Grad}_\alpha(\cdot)$" denotes the partial derivative of $(\cdot)$ with respect to the reference position $\mathbf{X}_\alpha$ of φ^α. Since the motion of any constituent φ^α was assumed to be unique and uniquely invertible with a non-zero Jacobian J_α, the domain of $\det \mathbf{F}_\alpha$ is restricted to positive values

$$\det \mathbf{F}_\alpha = J_\alpha > 0, \tag{18}$$

where, in the undeformed state, $\det \mathbf{F}_\alpha(t_0) = 1$ has been considered.

Concerning the definition of solid strain measures, a standard representation is given, e.g., by the introduction of the Green-Lagrangean strain $\mathbf{E}_S$ corresponding to the kinematics of the solid reference configuration or the Karni-Reiner strain $\mathbf{K}_S$ of the actual configuration, respectively:

$$\mathbf{E}_S = \frac{1}{2}(\mathbf{C}_S - \mathbf{I}), \quad \mathbf{K}_S = \frac{1}{2}(\mathbf{B}_S - \mathbf{I}). \tag{19}$$

Therein, $\mathbf{I}$ is the fundamental tensor of second order (second order identity) and

$$\mathbf{C}_S = \mathbf{F}_S^T \mathbf{F}_S, \quad \mathbf{B}_S = \mathbf{F}_S \mathbf{F}_S^T \tag{20}$$

are the right and left Green deformation tensors related to each other by the push-forward rotation $\mathbf{B}_S = \mathbf{R}_S \mathbf{C}_S \mathbf{R}_S^T$. Therein, $(\cdot)^T$ characterises the transposition of $(\cdot)$ and $\mathbf{R}_S$ is the continuum rotation of the polar decomposition of the deformation gradient. For an extended view on porous media kinematics including micropolar information, the interested reader is referred to [19].

In addition to the above strain measures based on the deformation gradient $\mathbf{F}_S$,

$$(\mathbf{F}_\alpha)'_\alpha = \mathrm{Grad}_\alpha \mathbf{x}'_\alpha \quad \text{and}$$
$$\mathbf{L}_\alpha = (\mathbf{F}_\alpha)'_\alpha \mathbf{F}_\alpha^{-1} = \mathrm{grad}\, \mathbf{x}'_\alpha \tag{21}$$

are the material and the spatial velocity gradients.

4 Balance relations

4.1 General frame

The discussion of balance relations for multiphasic and multicomponent materials is based on Truesdell's "metaphysical principles" of mixture theories, cf. Truesdell [55, p. 221]):

1. All properties of the mixture must be mathematical consequences of properties of the constituents.
2. So as to describe the motion of a constituent, we may in imagination isolate it from the rest of the mixture, provided we allow properly for the actions of the other constituents upon it.
3. The motion of the mixture is governed by the same equations as is a single body.

The foundation of Truesdell's principles proceeds from the idea that both the balance relations of the constituents φ^α and the balance relations of the overall medium (the mixture) $\varphi = \bigcup_{\alpha=1}^{k} \varphi^\alpha$ can be given in analogy to the balance relations of classical continuum mechanics of single-phase materials, provided one allows for the interaction mechanisms between the constituents by the introduction of so-called production terms.

4.2 Balance relations of the overall aggregate

Following this, the general balance relations for the overall aggregate φ can be directly given from the results of classical continuum mechanics of single-phase media:

$$\begin{aligned} \frac{\mathrm{d}}{\mathrm{d}t} \int_{\mathscr{B}} \Psi \, \mathrm{d}v &= \int_{\mathscr{S}} (\boldsymbol{\phi} \cdot \mathbf{n}) \, \mathrm{d}a + \int_{\mathscr{B}} \sigma \, \mathrm{d}v + \int_{\mathscr{B}} \hat{\Psi} \, \mathrm{d}v, \\ \frac{\mathrm{d}}{\mathrm{d}t} \int_{\mathscr{B}} \boldsymbol{\Psi} \, \mathrm{d}v &= \int_{\mathscr{S}} (\boldsymbol{\Phi}\, \mathbf{n}) \, \mathrm{d}a + \int_{\mathscr{B}} \boldsymbol{\sigma} \, \mathrm{d}v + \int_{\mathscr{B}} \hat{\boldsymbol{\Psi}} \, \mathrm{d}v. \end{aligned} \tag{22}$$

In the above equations, Ψ or $\boldsymbol{\Psi}$, respectively, are the volume-specific scalar- or vector-valued densities of the mechanical quantities in $\mathscr{B}$ to be balanced. In the framework of a general thermodynamical description, these quantities are given by the mass density, the linear momentum, the moment of momentum (angular momentum), the total energy (internal and kinetic) and the entropy. The quantities $\boldsymbol{\phi} \cdot \mathbf{n}$ and $\boldsymbol{\Phi}\, \mathbf{n}$, respectively, are the densities at the surface $\mathscr{S}$ of $\mathscr{B}$ (effluxes) of the mechanical quantities resulting from the external vicinity. Furthermore, $\mathbf{n}$ is the outward-oriented unit surface normal. σ or $\boldsymbol{\sigma}$, respectively, are the supply terms of the mechanical quantities resulting from the external distance, whereas $\hat{\Psi}$ or $\hat{\boldsymbol{\Psi}}$, respectively, are the production terms of the mechanical quantities as a result of possible couplings of φ with the surrounding of φ. Assuming steady and steadily differentiable integrands, differentiation of the left-hand side

of (22) and transformation of the surface integrals incorporated in the right-hand side of (22) into volume integrals yields the local forms of the balance relations, viz.:

$$\begin{aligned} \dot{\Psi} + \Psi \operatorname{div} \dot{\mathbf{x}} &= \operatorname{div} \boldsymbol{\phi} + \sigma + \hat{\Psi}, \\ \dot{\boldsymbol{\Psi}} + \boldsymbol{\Psi} \operatorname{div} \dot{\mathbf{x}} &= \operatorname{div} \boldsymbol{\Phi} + \boldsymbol{\sigma} + \hat{\boldsymbol{\Psi}}. \end{aligned} \tag{23}$$

Therein, the barycentric derivative (mixture derivative) $\overset{\cdot}{(\cdot)}$ is defined as follows:

$$\overset{\cdot}{(\cdot)} := \frac{\mathrm{d}(\cdot)}{\mathrm{d}t} = \frac{\partial (\cdot)}{\partial t} + \operatorname{grad}(\cdot) \cdot \dot{\mathbf{x}}\,. \tag{24}$$

Note that the barycentric velocity $\dot{\mathbf{x}}$ is given in analogy to (16), however, for the whole medium via

$$\dot{\mathbf{x}} = \frac{1}{\rho} \sum_{\beta=1}^{k} \rho^{\alpha} \mathbf{x}'_{\alpha}\,, \quad \text{where} \quad \rho = \sum_{\alpha=1}^{k} \rho^{\alpha} \tag{25}$$

is the density of the whole aggregate (mixture density). By taking the time derivative of $(25)_1$ following the barycentric motion of the mixture, one obtains the barycentric acceleration as

$$\ddot{\mathbf{x}} = \frac{1}{\rho} \sum_{\beta=1}^{k} \left[\rho^{\alpha} \overset{\prime\prime}{\mathbf{x}}_{\alpha} - \operatorname{div} (\rho^{\alpha} \mathbf{d}_{\alpha} \otimes \mathbf{d}_{\alpha}) + \hat{\rho}^{\alpha} \right], \tag{26}$$

where the diffusion velocities

$$\mathbf{d}_{\alpha} = \mathbf{x}'_{\alpha} - \dot{\mathbf{x}} \quad \text{with} \quad \sum_{\alpha=1}^{k} \rho^{\alpha} \mathbf{d}_{\alpha} = \mathbf{0} \tag{27}$$

have been used. The specific balance equations of mass, linear momentum, moment of momentum (m. o. m.), energy and entropy are introduced, as is usual in continuum thermodynamics, via axioms, thus leading to the representation given in Table 1. Therein, $\mathbf{T}$ is the Cauchy stress tensor and $\mathbf{b}$ the external volume force per unit mass or the gravitation, respectively. Furthermore, $\rho\, \dot{\mathbf{x}}$ is the momentum of the overall medium, whereas $\mathbf{x} \times (\rho\, \dot{\mathbf{x}})$ is the moment of momentum. Concerning the energy and entropy balance relations, ε is the internal energy, $\mathbf{q}$ is the heat influx vector, and r is the external heat supply. In addition, η is the entropy, $\boldsymbol{\phi}_{\boldsymbol{\eta}}$ and σ_{η} are the efflux of entropy and the external entropy supply, whereas $\hat{\eta}$ is the non-negative entropy production [18].

Inserting the quantities given in Table 1 into the local balances (23), one obtains with the aid of the respective "lower" balances the following relations known from continuum mechanics of single-phase materials, cf. e.g. [18, 40]:

$$\begin{aligned} &\bullet \text{ mass:} && \dot{\rho} + \rho \operatorname{div} \dot{\mathbf{x}} = 0\,, \\ &\bullet \text{ momentum:} && \rho\, \ddot{\mathbf{x}} = \operatorname{div} \mathbf{T} + \rho\, \mathbf{b}\,, \\ &\bullet \text{ m. o. m.:} && \mathbf{0} = \mathbf{I} \times \mathbf{T} \;\longrightarrow\; \mathbf{T} = \mathbf{T}^{T}, \\ &\bullet \text{ energy:} && \rho\, \dot{\varepsilon} = \mathbf{T} \cdot \mathbf{L} - \operatorname{div} \mathbf{q} + \rho\, r\,, \\ &\bullet \text{ entropy:} && \rho\, \dot{\eta} \geq \operatorname{div} \boldsymbol{\phi}_{\boldsymbol{\eta}} + \sigma_{\eta}\,. \end{aligned} \tag{28}$$

In the framework of single-phase materials, it is usual (and correct) to proceed from the following a priori constitutive assumptions for the entropy efflux and the entropy supply,

$$\boldsymbol{\phi}_{\boldsymbol{\eta}} = -\frac{1}{\theta}\, \mathbf{q}\,, \quad \sigma_{\eta} = \frac{1}{\theta}\, \rho\, r\,, \tag{29}$$

where θ is the absolute Kelvin's temperature. Given (29), the entropy relation $(28)_5$ reads

$$\rho\, \dot{\eta} \geq \operatorname{div} \left(-\frac{1}{\theta}\, \mathbf{q} \right) + \frac{1}{\theta}\, \rho\, r\,. \tag{30}$$

However, transferring this result to multiphasic materials leads to a wrong result and can hence not be used. This problem, by the way, gave rise to considerable irritations in the literature on mixture theories in the sixties of the last century, cf. Ehlers [15].

4.3 Balance relations of the constituents

Following Truesdell's principles, the general balance relations of a constituent φ^{α} of the overall medium φ yield in analogy to (22):

$$\begin{aligned} &\frac{\mathrm{d}_{\alpha}}{\mathrm{d}t} \int_{\mathscr{B}} \Psi^{\alpha}\, \mathrm{d}v \\ &\quad = \int_{\mathscr{S}} (\boldsymbol{\phi}^{\boldsymbol{\alpha}} \cdot \mathbf{n})\; \mathrm{d}a + \int_{\mathscr{B}} \sigma^{\alpha}\, \mathrm{d}v + \int_{\mathscr{B}} \hat{\Psi}^{\alpha}\, \mathrm{d}v, \\ &\frac{\mathrm{d}_{\alpha}}{\mathrm{d}t} \int_{\mathscr{B}} \boldsymbol{\Psi}^{\boldsymbol{\alpha}}\, \mathrm{d}v \\ &\quad = \int_{\mathscr{S}} (\boldsymbol{\Phi}^{\boldsymbol{\alpha}}\, \mathbf{n})\; \mathrm{d}a + \int_{\mathscr{B}} \boldsymbol{\sigma}^{\boldsymbol{\alpha}}\, \mathrm{d}v + \int_{\mathscr{B}} \hat{\boldsymbol{\Psi}}^{\boldsymbol{\alpha}}\, \mathrm{d}v. \end{aligned} \tag{31}$$

Therein, the mechanical quantities $(\cdot)^{\alpha}$ have the same physical meaning as the quantities $(\cdot)$ included into (22). Differentiation of the left-hand side of (31) and transformation of the surface integrals into volume integrals yields the local forms

$$\begin{aligned} (\Psi^{\alpha})'_{\alpha} + \Psi^{\alpha} \operatorname{div} \mathbf{x}'_{\alpha} &= \operatorname{div}\, \boldsymbol{\phi}^{\boldsymbol{\alpha}} + \sigma^{\alpha} + \hat{\Psi}^{\alpha}, \\ (\boldsymbol{\Psi}^{\boldsymbol{\alpha}})'_{\alpha} + \boldsymbol{\Psi}^{\boldsymbol{\alpha}} \operatorname{div} \mathbf{x}'_{\alpha} &= \operatorname{div}\, \boldsymbol{\Phi}^{\boldsymbol{\alpha}} + \boldsymbol{\sigma}^{\boldsymbol{\alpha}} + \hat{\boldsymbol{\Psi}}^{\boldsymbol{\alpha}}. \end{aligned} \tag{32}$$

From Truesdell's metaphysical principles, the local balances of the overall medium φ are given, on the one hand, by the balance relations (23) of single-phase media. On the other hand, these balance equations can be obtained by the sum of the balance relations (32) over all k constituents φ^{α}. This statement leads to constraints expressed by sum

Table 1 Balance relations for the overall medium φ

	Ψ, Ψ	ϕ, Φ	σ, σ	$\hat{\Psi}$, $\hat{\Psi}$
mass	ρ	$\mathbf{0}$	0	0
momentum	$\rho\,\dot{\mathbf{x}}$	$\mathbf{T}$	$\rho\,\mathbf{b}$	$\mathbf{0}$
m. o. m.	$\mathbf{x}\times(\rho\,\dot{\mathbf{x}})$	$\mathbf{x}\times\mathbf{T}$	$\mathbf{x}\times(\rho\,\mathbf{b})$	$\mathbf{0}$
energy	$\rho\,\varepsilon+\frac{1}{2}\,\dot{\mathbf{x}}\cdot(\rho\,\dot{\mathbf{x}})$	$\mathbf{T}^T\,\dot{\mathbf{x}}-\mathbf{q}$	$\dot{\mathbf{x}}\cdot(\rho\,\mathbf{b})+\rho\,r$	0
entropy	$\rho\,\eta$	ϕ_η	σ_η	$\hat{\eta}$

Table 2 Balance relations for a constituent φ^α of the overall medium φ

	Ψ^α, Ψ^α	ϕ^α, ϕ^α	σ^α, σ^α	$\hat{\Psi}^\alpha$, $\hat{\Psi}^\alpha$
mass	ρ^α	$\mathbf{0}$	0	$\hat{\rho}^\alpha$
momentum	$\rho^\alpha\mathbf{x}'_\alpha$	$\mathbf{T}^\alpha$	$\rho^\alpha\mathbf{b}^\alpha$	$\hat{\mathbf{s}}^\alpha$
m. o. m.	$\mathbf{x}\times(\rho^\alpha\mathbf{x}'_\alpha)$	$\mathbf{x}\times\mathbf{T}^\alpha$	$\mathbf{x}\times(\rho^\alpha\mathbf{b}^\alpha)$	$\hat{\mathbf{h}}^\alpha$
energy	$\rho^\alpha\varepsilon^\alpha+\frac{1}{2}\mathbf{x}'_\alpha\cdot(\rho^\alpha\mathbf{x}'_\alpha)$	$(\mathbf{T}^\alpha)^T\mathbf{x}'_\alpha-\mathbf{q}^\alpha$	$\mathbf{x}'_\alpha s\cdot(\rho^\alpha\mathbf{b}^\alpha)+\rho^\alpha r^\alpha$	$\hat{e}^\alpha$
entropy	$\rho^\alpha\,\eta^\alpha$	ϕ^α_η	σ^α_η	$\hat{\eta}^\alpha$

relations which, e.g. for scalar-valued mechanical quantities, read:

- mechanical quantity: $\Psi=\sum_{\alpha=1}^{k}\Psi^\alpha$,
- efflux: $\phi\cdot\mathbf{n}=\sum_{\alpha=1}^{k}[\phi^\alpha-\Psi^\alpha(\mathbf{x}'_\alpha-\dot{\mathbf{x}})]\cdot\mathbf{n}$, (33)
- supply: $\sigma=\sum_{\alpha=1}^{k}\sigma^\alpha$,
- production: $\hat{\Psi}=\sum_{\alpha=1}^{k}\hat{\Psi}^\alpha$.

Concerning vector-valued mechanical quantities, one analogously obtains

- mechanical quantity: $\Psi=\sum_{\alpha=1}^{k}\Psi^\alpha$,
- efflux: $\Phi\,\mathbf{n}=\sum_{\alpha=1}^{k}[\Phi^\alpha-\Psi^\alpha\otimes(\mathbf{x}'_\alpha-\dot{\mathbf{x}})]\mathbf{n}$, (34)
- supply: $\sigma=\sum_{\alpha=1}^{k}\sigma^\alpha$,
- production: $\hat{\Psi}=\sum_{\alpha=1}^{k}\hat{\Psi}^\alpha$.

The individual balance equations of mass, momentum, moment of momentum, energy and entropy are obtained in direct analogy to those of single-phase materials provided one allows for the interaction mechanisms between the constituents by introducing additional production terms. The quantities $(\cdot)^\alpha$ included into the balance relations of φ^α, cf. Table 2, have the same physical meaning as the corresponding quantities $(\cdot)$ of φ incorporated into Table 1. Furthermore, the mass production $\hat{\rho}^\alpha$ allows for mass exchange or phase transition processes between the constituents, $\hat{\mathbf{s}}^\alpha$ is the total momentum production of φ^α, and $\hat{\mathbf{h}}^\alpha$ represents the total moment of momentum production, whereas $\hat{e}^\alpha$ is the total energy production term. Finally, $\hat{\eta}^\alpha$ is the total entropy production of φ^α.

In the same way, as it was assumed in the theory of single-phase materials, cf. (29), it is possible (and correct) to specify the efflux of entropy and the external entropy supply of any constituent φ^α as

$$\phi^\alpha_\eta=-\frac{1}{\theta^\alpha}\,\mathbf{q}^\alpha,\quad \sigma^\alpha_\eta=\frac{1}{\theta^\alpha}\,\rho^\alpha r^\alpha. \tag{35}$$

Admitting different Kelvin's temperatures θ^α in the above constitutive assumptions, one allows for the possibility that each constituent has an individual temperature function.

In the framework of multi-component materials as well as in mixture theories, the total productions can be split into a direct term and additional terms governed by the "lower" productions. Thus,

$$\begin{aligned}
\hat{\mathbf{s}}^\alpha&=\hat{\mathbf{p}}^\alpha+\hat{\rho}^\alpha\mathbf{x}'_\alpha,\\
\hat{\mathbf{h}}^\alpha&=\hat{\mathbf{m}}^\alpha+\mathbf{x}\times(\hat{\mathbf{p}}^\alpha+\hat{\rho}^\alpha\mathbf{x}'_\alpha),\\
\hat{e}^\alpha&=\hat{\varepsilon}^\alpha+\hat{\mathbf{p}}^\alpha\cdot\mathbf{x}'_\alpha+\hat{\rho}^\alpha\left(\varepsilon^\alpha+\frac{1}{2}\mathbf{x}'_\alpha\cdot\mathbf{x}'_\alpha\right),\\
\hat{\eta}^\alpha&=\hat{\zeta}^\alpha+\hat{\rho}^\alpha\eta^\alpha.
\end{aligned} \tag{36}$$

In $(36)_1$, the direct momentum production $\hat{\mathbf{p}}^\alpha$ can be interpreted as the local interaction force per unit volume between

φ^α and the other constituents of the overall medium, whereas the second term represents the additional momentum production as a result of the density production term. Analogously, $\hat{\mathbf{m}}^\alpha$ is the direct part of the total moment of momentum production $\hat{\mathbf{h}}^\alpha$, whereas the further terms represent the additional productions of angular momentum resulting from the direct momentum production and the density production. Furthermore, $\hat{\varepsilon}^\alpha$ is the direct energy production term included into the total energy production $\hat{e}^\alpha$, whereas the remainder of terms represents the additional energy production stemming from the momentum and the density productions, respectively.

Using the same procedure as to obtain (28) from Table 1, one obtains the following equations from Table 2 using the above additive split of the production terms:

$$
\begin{aligned}
&\bullet \text{ mass:} && (\rho^\alpha)'_\alpha + \rho^\alpha \operatorname{div} \mathbf{x}'_\alpha = \hat{\rho}^\alpha,\\
&\bullet \text{ momentum:} && \rho^\alpha \, \mathbf{x}''_\alpha = \operatorname{div} \mathbf{T}^\alpha + \rho^\alpha \mathbf{b}^\alpha + \hat{\mathbf{p}}^\alpha,\\
&\bullet \text{ m. o. m.:} && \mathbf{0} = \mathbf{I} \times \mathbf{T}^\alpha + \hat{\mathbf{m}}^\alpha,\\
&\bullet \text{ energy:} && \rho^\alpha (\varepsilon^\alpha)'_\alpha = \mathbf{T}^\alpha \cdot \mathbf{L}_\alpha - \operatorname{div} \mathbf{q}^\alpha \\
& && \qquad + \rho^\alpha r^\alpha + \hat{\varepsilon}^\alpha,\\
&\bullet \text{ entropy:} && \rho^\alpha (\eta^\alpha)'_\alpha = \operatorname{div} \left(-\frac{1}{\theta^\alpha} \mathbf{q}^\alpha \right) \\
& && \qquad + \frac{1}{\theta^\alpha} \rho^\alpha r^\alpha + \hat{\zeta}^\alpha .
\end{aligned}
\tag{37}
$$

By summing up the relations (37) over the k constituents φ^α, one obtains the following constraints of the production terms in comparison with the relations (28) of the overall medium φ:

$$
\begin{aligned}
&\sum_{\alpha=1}^{k} \hat{\rho}^\alpha = 0, \quad \sum_{\alpha=1}^{k} \hat{\mathbf{s}}^\alpha = \mathbf{0}, \quad \sum_{\alpha=1}^{k} \hat{\mathbf{h}}^\alpha = \mathbf{0},\\
&\sum_{\alpha=1}^{k} \hat{e}^\alpha = 0, \quad \sum_{\alpha=1}^{k} \hat{\eta}^\alpha \geq 0.
\end{aligned}
\tag{38}
$$

Proceeding from the general constraints given by (36), the explicit relations between the total quantities of Table 1 and the partial quantities of Table 2 read

$$
\begin{aligned}
\rho \, \mathbf{b} &= \sum_{\alpha=1}^{k} \rho^\alpha \mathbf{b}^\alpha ,\\
\mathbf{T} &= \sum_{\alpha=1}^{k} \left(\mathbf{T}^\alpha - \rho^\alpha \mathbf{d}_\alpha \otimes \mathbf{d}_\alpha \right),\\
\rho \, \varepsilon &= \sum_{\alpha=1}^{k} \rho^\alpha \left(\varepsilon^\alpha + \frac{1}{2} \mathbf{d}_\alpha \cdot \mathbf{d}_\alpha \right),\\
\mathbf{q} &= \sum_{\alpha=1}^{k} \Big[\mathbf{q}^\alpha - (\mathbf{T}^\alpha)^T \mathbf{d}_\alpha + \rho^\alpha \varepsilon^\alpha \mathbf{d}_\alpha \\
&\qquad + \frac{1}{2} \rho^\alpha (\mathbf{d}_\alpha \cdot \mathbf{d}_\alpha) \mathbf{d}_\alpha \Big],\\
\rho \, r &= \sum_{\alpha=1}^{k} \rho^\alpha (r^\alpha + \mathbf{b}^\alpha \cdot \mathbf{d}_\alpha),\\
\rho \, \eta &= \sum_{\alpha=1}^{k} \rho^\alpha \eta^\alpha ,
\end{aligned}
\tag{39}
$$

where to obtain $(39)_{2-5}$, the diffusion velocities $\mathbf{d}_\alpha$ have been used. The sum relations included in (39) can be interpreted as follows:

- As far as there is no diffusion process ($\mathbf{d}_\alpha = \mathbf{0}$), all terms of the overall medium are given by summing up the respective terms of the constituents.
- In case that there is a diffusion process ($\mathbf{d}_\alpha \neq \mathbf{0}$), summing up $\mathbf{T}^\alpha$, $\rho^\alpha \varepsilon^\alpha$, $\mathbf{q}^\alpha$ and $\rho^\alpha r^\alpha$ yields the so-called inner parts (kernels) of $\mathbf{T}$, $\rho \, \varepsilon$, $\mathbf{q}$ and $\rho \, r$. The remainder of terms included in the sum relations are governed by the diffusion process through $\mathbf{d}_\alpha$. These terms can be interpreted as follows: That part of the stress tensor $\mathbf{T}$ that is initiated, for a given constituent φ^α, by the diffusion process is comparable to the Reynolds stress occurring in turbulent flow situations of single-constituent fluids. Furthermore, the volume-specific internal energy $\rho \, \varepsilon$ contains the diffusive kinetic energy of the constituents. The non-mechanical influx vector $\mathbf{q}$ is influenced by the sum of the influx terms generated by the diffusive work of the partial contact forces as well as by the influx vectors generated by the diffusive internal and kinetic energies. Finally, the non-mechanical supply term $\rho \, r$ contains additional terms which stem from the diffusive work of the external volume forces.

Given the relations (37)–(39), the entropy principle for mixtures and multiphasic porous media models yields

$$
\begin{aligned}
&\sum_{\alpha=1}^{k} \Big[\rho^\alpha (\eta^\alpha)'_\alpha + \hat{\rho}^\alpha \eta^\alpha \\
&\quad + \operatorname{div} \left(\frac{1}{\theta^\alpha} \mathbf{q}^\alpha \right) - \frac{1}{\theta^\alpha} \rho^\alpha r^\alpha \Big] \geq 0.
\end{aligned}
\tag{40}
$$

Applying the mixture derivative defined by (24) to the entropy functions η^α, one obtains with the aid of $(39)_6$ instead of (40)

$$
\rho \, \dot{\eta} \geq \sum_{\alpha=1}^{k} \operatorname{div} \left(\frac{1}{\theta^\alpha} \mathbf{q}^\alpha - \rho^\alpha \eta^\alpha \mathbf{d}_\alpha \right) + \sum_{\alpha=1}^{k} \frac{1}{\theta^\alpha} \rho^\alpha r^\alpha . \tag{41}
$$

This form of the entropy principle can easily be compared with the entropy inequality (30) for single-phase materials. Following this, it is concluded that

$$\boldsymbol{\phi_\eta} = -\sum_{\alpha=1}^{k}\left(\frac{1}{\theta^\alpha}\mathbf{q}^\alpha + \rho^\alpha\eta^\alpha\mathbf{d}_\alpha\right) \quad \text{and}$$

$$\sigma_\eta = \sum_{\alpha=1}^{k}\frac{1}{\theta^\alpha}\rho^\alpha r^\alpha . \tag{42}$$

Given (42), it is immediately seen that the sum relations defined by (33) are also valid for the entropy flux and the entropy supply term. In comparison to the relations (35) and (42), it is furthermore seen that the entropy principles for single-phase and multiphasic materials only leads to the same inequalities if the diffusion process vanishes ($\mathbf{d}_\alpha = \mathbf{0}$) and if all constituents φ^α additionally have the same Kelvin's temperature ($\theta^\alpha \equiv \theta$).

Introducing mass-specific constituent free energy functions ψ^α via

$$\psi^\alpha := \varepsilon^\alpha - \theta^\alpha\eta^\alpha , \tag{43}$$

one obtains with the aid of the energy balance relations $(37)_3$ the mostly used form of the entropy principle for multiphasic materials, viz.:

$$\sum_{\alpha=1}^{k}\frac{1}{\theta^\alpha}\Big[\mathbf{T}^\alpha\cdot\mathbf{L}_\alpha - \rho^\alpha[(\psi^\alpha)'_\alpha + (\theta^\alpha)'_\alpha\eta^\alpha] - \hat{\mathbf{p}}^\alpha\cdot\mathbf{x}'_\alpha - \hat{\rho}^\alpha(\psi^\alpha + \tfrac{1}{2}\mathbf{x}'_\alpha\cdot\mathbf{x}'_\alpha) - \frac{1}{\theta^\alpha}\mathbf{q}^\alpha\cdot\operatorname{grad}\theta^\alpha + \hat{e}^\alpha\Big] \geq 0. \tag{44}$$

In case of single-temperature problems ($\theta^\alpha \equiv \theta$), the above inequality can be multiplied by θ. Then,

$$\sum_{\alpha=1}^{k}[\mathbf{T}^\alpha\cdot\mathbf{L}_\alpha - \rho^\alpha(\psi^\alpha)'_\alpha - \hat{\mathbf{p}}^\alpha\cdot\mathbf{x}'_\alpha - \hat{\rho}^\alpha \times(\psi^\alpha + \tfrac{1}{2}\mathbf{x}'_\alpha\cdot\mathbf{x}'_\alpha)] - \rho\eta\,\dot{\theta} - \frac{1}{\theta}\mathbf{h}\cdot\operatorname{grad}\theta \geq 0, \tag{45}$$

where $(38)_4$ together with the definitions

$$\mathbf{h} := \sum_{\alpha=1}^{k}\mathbf{h}^\alpha \quad \text{and} \quad \mathbf{h}^\alpha := \mathbf{q}^\alpha + \theta\rho^\alpha\eta^\alpha\mathbf{d}_\alpha \tag{46}$$

has been used.

5 Constitutive models and basic numerical setting

5.1 General framework

Any kind of porous media model can be embedded in the framework discussed above. However, depending on the problem at hand, additional information is necessary. With respect to the broad variety of problems that can be discussed within the TPM, it is evident that only a very small selection can be discussed within this article. Following this, two basic problems will be considered. The first one, as a fundamental geotechnical problem, concerns the mechanics of unsaturated soil, while the second one describes the possibilities of electro-active polymers and gels and can easily be reduced to swelling phenomena of active soil and biological tissue. Various further applications can be taken from the literature [8,37,43,60,61] and from the work of the author and coworkers, cf. e.g. [21–32]. While the first example proceeds from small deformation of an elasto-plastic soil with an immiscible combination of a fluid and a gaseous pore content, the second one depends on finite elastic deformations of swelling media driven through osmosis and electro-chemical effects. Furthermore, to realise swelling phenomena, there are fixed charges adhering at the solid material, while the pore content is a real mixture of a liquid solute with positively and negatively charged ions as solutes. Both examples will be discussed within a framework of isothermal processes, for non-isothermal circumstances, cf. e.g. the dissertation theses by Ghadiani [38] and Graf [39].

5.2 Unsaturated soil as a triphasic material

General setting. Based on the balance equations $(37)_{1,2}$, a triphasic material composed of a soil skeleton φ^S and an immiscible pore content φ^F consisting of a pore liquid (water) φ^L and a pore gas (air) φ^G is governed by the following mass and momentum balances:

$$\left.\begin{aligned}&(\rho^\alpha)'_\alpha + \rho^\alpha\operatorname{div}\mathbf{x}'_\alpha = 0,\\ &\mathbf{0} = \operatorname{div}\mathbf{T}^\alpha + \rho^\alpha\mathbf{b}^\alpha + \hat{\mathbf{p}}^\alpha\end{aligned}\right\} \quad \alpha = \{S,\, L,\, G\}$$

$$\text{and} \quad \varphi^F = \bigcup_{\beta=L,G}\varphi^\beta . \tag{47}$$

To obtain (47), it has been assumed, firstly, that only quasi-static processes ($\overset{\prime\prime}{\mathbf{x}}_\alpha = \mathbf{0}$) have to be considered and that, secondly, phase transitions can be excluded at ambient temperature conditions such that there is no water vaporisation/condensation or freezing/melting. As a result, mass exchanges between the constituents can be excluded such that the density productions $\hat{\rho}^\alpha$ vanish.

Furthermore, as a result of $(37)_3$ combined with the effect of symmetric stresses at the micro-structure of the individual components yielding $\hat{\mathbf{m}}^\alpha$ to vanish, cf. [19], it is assumed that

$$\mathbf{T}^\alpha = (\mathbf{T}^\alpha)^T, \tag{48}$$

also cf. $(28)_3$. As a result of $(36)_1$ and $(38)_2$, the direct momentum productions $\hat{\mathbf{p}}^\alpha$ or the local interaction forces between the constituents φ^α, respectively, are constrained by

$$\hat{\mathbf{p}}^S + \hat{\mathbf{p}}^F = \mathbf{0}, \quad \text{where} \quad \hat{\mathbf{p}}^F = \hat{\mathbf{p}}^L + \hat{\mathbf{p}}^G. \tag{49}$$

Assuming the solid material as well as the pore liquid to be materially incompressible ($\rho^{\alpha R} = \text{const.}$), the mass balance equation $(47)_1$ reduces to the volume balance

$$(n^\alpha)'_\alpha + n^\alpha \operatorname{div} \mathbf{x}'_\alpha = 0 \quad \text{with} \quad \alpha = \{S,\, L\}. \tag{50}$$

In case of the skeleton material, an integration of (50) leads to

$$n^S = n^S_{0S} \left(\det \mathbf{F}_S\right)^{-1}, \tag{51}$$

which, in the framework of a small strain approach, can be formally linearised around the natural state of φ^S to yield

$$n^S = n^S_{0S} \left(1 - \operatorname{Div}_S \mathbf{u}_S\right). \tag{52}$$

Therein, $\operatorname{Div}_S(\cdot)$ is the divergence operator corresponding to $\operatorname{Grad}_S(\cdot)$. Furthermore, n^S_{0S} is the volume fraction of φ^S in the solid reference configuration at time $t = t_0$. Note in passing that, in case of a small strain approach, it is generally not necessary to distinguish between $\operatorname{Grad}_S(\cdot)$ and $\operatorname{grad}(\cdot)$ or between $\operatorname{Div}_S(\cdot)$ and $\operatorname{div}(\cdot)$. Consequently, the remainder of this article is based on spatial gradient and divergence operators.

Given (51) or (52), the overall fluid volume fraction n^F (porosity) is coupled with the solid deformation by the solid volume fraction n^S via the saturation condition (4). However, to determine the portions of the liquid and the gas constituents, an additional constitutive equation for the liquid saturation function s^L or for the gas saturation function s^G, respectively, is required such that n^L and n^G can be determined through $(7)_2$ together with

$$\begin{aligned} &n^F = n^L + n^G \quad \text{with} \quad n^L = s^L n^F \quad \text{and} \\ &n^G = s^G n^F, \quad \text{where} \quad s^G = 1 - s^L. \end{aligned} \tag{53}$$

Proceeding from an isothermal triphasic formulation of partially saturated soil, any computational procedure is based on a basic set of five primary variables given by the solid displacement $\mathbf{u}_S$, the seepage velocities $\mathbf{w}_L$ and $\mathbf{w}_G$ and the effective pore-fluid pressures p^{LR} and p^{GR}. Under quasi-static conditions, one obtains a coupling between the seepage velocities and the effective liquid and gas pressures resulting from the individual fluid momentum balances and the constitutive setting yielding Darcy-like relations. Following this reduces the set of primary variables from five to three: the solid displacement $\mathbf{u}_S$ and the effective pressures p^{LR} and p^{GR}. The corresponding set of governing equations is then given by the vector-valued overall momentum balance corresponding to $\mathbf{u}_S$ and the scalar-valued liquid volume and gas mass balance equations corresponding to p^{LR} and p^{GR}. Thus,

$$\begin{aligned} \mathbf{0} &= \operatorname{div} \mathbf{T} + \rho\, \mathbf{g}, \\ 0 &= (n^L)'_S + n^L \operatorname{div} (\mathbf{u}_S)'_S + \operatorname{div} (n^L \mathbf{w}_L), \\ 0 &= n^G (\rho^{GR})'_S + (n^G)'_S \rho^{GR} + n^G \rho^{GR} \operatorname{div} (\mathbf{u}_S)'_S \\ &\quad + \operatorname{div} (n^G \rho^{GR} \mathbf{w}_G). \end{aligned} \tag{54}$$

Therein, $(54)_1$ has been obtained by taking the sum of the momentum balances $(47)_2$ of φ^S, φ^L and φ^G, where the constraint (49) has been taken into consideration together with the assumption of a constant gravitational force $\mathbf{g}$ such that $\mathbf{b}^\alpha = \mathbf{b} \equiv \mathbf{g}$. Furthermore,

$$\begin{aligned} &\mathbf{T} = \mathbf{T}^S + \mathbf{T}^L + \mathbf{T}^G, \\ &\rho = n^S \rho^{SR} + n^L \rho^{LR} + n^G \rho^{GR} \end{aligned} \tag{55}$$

define the overall Cauchy stress and the overall density of the triphasic material, cf. (6) and $(39)_2$. Summing over $\mathbf{T}^\alpha$ yields the kernel of the total stress $\mathbf{T}$ which, in case of quasi-static situations, is identical to $\mathbf{T}$ itself, since the diffusive parts included in $\operatorname{div} \mathbf{T}$ as well as those included in $\ddot{\mathbf{x}}$ drop off, cf. (26) in combination with $(39)_2$. Furthermore, note in passing that, by use of $(6)_2$ and (50), the last two balances of (54) are written with respect to the skeleton motion, where, additionally, on the basis of (14) and $(15)_2$,

$$\mathbf{x}'_\beta = \mathbf{x}'_S + (\operatorname{grad} \mathbf{x}'_\beta)\, \mathbf{w}_\beta \quad \text{with} \quad \beta = \{L,\, G\} \tag{56}$$

has been used.

Restrictions obtained from the entropy inequality. To close the triphasic model under consideration, constitutive equations are required for the partial Cauchy stresses $\mathbf{T}^\alpha$, the linear momentum productions $\hat{\mathbf{p}}^\beta$ of the pore fluids, the liquid saturation s^L and the effective gas pressure p^{GR}. However, since p^{GR} is assumed as a primary variable, the constitutive equation for p^{GR} will be inverted to yield an equation for the effective density ρ^{GR}.

Proceeding from standard arguments of Rational Thermodynamics, an evaluation of the overall entropy inequality

$$\begin{aligned} &\mathbf{T}^S \cdot \mathbf{L}_S - \rho^S (\psi^S)'_S + \mathbf{T}^L \cdot \mathbf{L}_L - \rho^L (\psi^L)'_L \\ &\quad + \mathbf{T}^G \cdot \mathbf{L}_G - \rho^G (\psi^G)'_G - \hat{\mathbf{p}}^L \cdot \mathbf{w}_L - \hat{\mathbf{p}}^G \cdot \mathbf{w}_G \geq 0 \end{aligned} \tag{57}$$

obtained from (45) for the triphasic model under consideration imposes the necessary thermodynamical restrictions on the process. However, since the process under discussion is constrained by the saturation condition (4), it is necessary to include this information into the entropy inequality. Taking the material time derivative of the saturation condition following the skeleton motion yields

$$\begin{aligned} \left(\sum_\alpha n^\alpha\right)'_S = -\Big[&n^S \operatorname{div} \mathbf{x}'_S + n^L \operatorname{div} \mathbf{x}'_L + n^G \operatorname{div} \mathbf{x}'_G \\ &+ \operatorname{grad} n^L \cdot \mathbf{w}_L + \operatorname{grad} n^G \cdot \mathbf{w}_G + \frac{n^G}{\rho^{GR}} (\rho^{GR})'_S \Big] \\ = 0, \end{aligned} \tag{58}$$

where $(47)_1$ and $(6)_2$ have been used for φ^G and (50) for φ^S and φ^L. Multiplying the saturation constraint (58) by a Lagrangean multiplier Λ and combining (57) with (58) transfers the entropy inequality to its final representation, viz.:

$$\begin{aligned}
&(\mathbf{T}^S + n^S \Lambda \mathbf{I}) \cdot \mathbf{L}_S - \rho^S (\psi^S)'_S \\
&\quad + (\mathbf{T}^L + n^L \Lambda \mathbf{I}) \cdot \mathbf{L}_L - \rho^L (\psi^L)'_L \\
&\quad + (\mathbf{T}^G + n^G \Lambda \mathbf{I}) \cdot \mathbf{L}_G - \rho^G (\psi^G)'_G \\
&\quad + \Lambda \frac{n^G}{\rho^{GR}} (\rho^{GR})'_G - (\hat{\mathbf{p}}^L - \Lambda \operatorname{grad} n^L) \cdot \mathbf{w}_L \\
&\quad - (\hat{\mathbf{p}}^G - \Lambda \operatorname{grad} n^G) \cdot \mathbf{w}_G \geq 0 \,. \qquad (59)
\end{aligned}$$

Evaluating (59) by use of the constitutive assumptions

$$\psi^S = \psi^S(\mathbf{F}_S), \quad \psi^L = \psi^L(s^L), \quad \psi^G = \psi^G(\rho^{GR}) \qquad (60)$$

yields with the aid of standard arguments (e.g. [10, 19, 39])

$$\begin{aligned}
\mathbf{T}^S &= -n^S p^{FR} \mathbf{I} + \mathbf{T}^S_E, \\
\mathbf{T}^G &= -n^G p^{GR} \mathbf{I} + \mathbf{T}^G_E, \\
\hat{\mathbf{p}}^G &= p^{GR} \operatorname{grad} n^G + \hat{\mathbf{p}}^G_E, \\
\mathbf{T}^L &= -n^L p^{LR} \mathbf{I} + \mathbf{T}^L_E, \\
\hat{\mathbf{p}}^L &= p^{LR} \operatorname{grad} n^L \\
&\quad + p^C [s^G \operatorname{grad} n^L - s^L \operatorname{grad} n^G] + \hat{\mathbf{p}}^L_E .
\end{aligned} \qquad (61)$$

Therein, the solid extra stress $\mathbf{T}^S_E$, the effective pore pressure $\mathscr{P} := p^{FR}$, the Lagrangean multiplier Λ and the capillary pressure p^C defined as the difference between the effective pressure p^{GR} of the non-wetting fluid, the gas, and the effective pressure p^{LR} of the wetting fluid, the liquid, are given by

$$\begin{aligned}
\mathbf{T}^S_E &= \rho^S \frac{\partial \psi^S}{\partial \mathbf{F}_S} \mathbf{F}_S^T , \\
\mathscr{P} &:= p^{FR} = s^L p^{LR} + s^G p^{GR} . \\
\Lambda &= p^{GR} = (\rho^{GR})^2 \frac{\partial \psi^G}{\partial \rho^{GR}} , \\
p^C &:= p^{GR} - p^{LR} = -s^L \rho^{LR} \frac{\partial \psi^L}{\partial s^L} .
\end{aligned} \qquad (62)$$

While $(62)_1$ describes the extra stress of an elastic porous solid, the viscous extra stresses of the fluid components, $\mathbf{T}^L_E$ and $\mathbf{T}^G_E$, are usually neglected in comparison with the extra momentum productions $\hat{\mathbf{p}}^L_E$ and $\hat{\mathbf{p}}^G_E$ resulting from local interaction forces between the constituents. Furthermore, note in passing that Dalton's law given by $\mathscr{P} = s^L p^{LR} + s^G p^{GR}$ was recovered by thermodynamical considerations. Moreover, as a result of the materially incompressible pore liquid, the effective liquid pressure p^{LR} acts as a Lagrangean and is thus determined by the boundary conditions of the problem under study. Finally, in the remainder of this section, the pressures p^{LR} and p^{GR} are understood as "effective excess pressures" exceeding a typical ambient pressure like, e.g., the atmospheric pressure p_0.

Finally, with the remarks given above, an addition of the constituent stresses $\mathbf{T}^\alpha$ yields

$$\mathbf{T} = -\mathscr{P} \mathbf{I} + \mathbf{T}^S_E , \qquad (63)$$

where $(55)_1$ has been used. Thus, the overall Cauchy stress $\mathbf{T}$ yields the well-known "concept of effective stress" [2, 19, 53], where, as is usual in geotechnical applications, the extra stress $\mathbf{T}^S_E$ is identified as the effective stress of a porous soil.

The fluid constituents. Concerning the fluid materials, liquid and gas, the extra momentum productions $\hat{\mathbf{p}}^L_E$ and $\hat{\mathbf{p}}^G_E$, the capillary pressure p^C and the effective gas pressure p^{GR} have to be specified by constitutive equations. As was mentioned before, the model under consideration proceeds from p^{GR} as a primary variable. Thus, $p^{GR} = p^{GR}(\rho^{GR})$ is needed in the inverse form $\rho^{GR} = \rho^{GR}(p^{GR})$. Analogously, one proceeds from $s^L = s^L(p^C)$ instead of $p^C = p^C(s^L)$.

A combination of (59) with the constitutive assumptions (60) and the results (61) and (62) yields the dissipation mechanism

$$\mathscr{D} = -\hat{\mathbf{p}}^L_E \cdot \mathbf{w}_G - \hat{\mathbf{p}}^G_E \cdot \mathbf{w}_G \geq 0 \,. \qquad (64)$$

Proceeding from

$$\hat{\mathbf{p}}^\beta_E = -(n^\beta)^2 \gamma^{\beta R} (\mathbf{K}^\beta_r)^{-1} \mathbf{w}_\beta , \qquad (65)$$

where $\gamma^{\beta R} = \rho^{\beta R} |\mathbf{g}|$ is the specific weight of φ^β ($\beta = \{L, G\}$) and $\mathbf{K}^\beta_r$ is the corresponding relative permeability tensor, yields the dissipation mechanism (64) to hold with positive definite permeabilities $\mathbf{K}^\beta_r$. Note that $\mathbf{K}^\beta_r$ is related to the Darcy permeability tensor $\mathbf{K}^\beta$ through

$$\mathbf{K}^\beta_r = \kappa^\beta_r \mathbf{K}^\beta . \qquad (66)$$

Therein, κ^β_r is the so-called relative permeability factor depending on the saturation of φ^β, whereas $\mathbf{K}^\beta$ is understood as the permeability tensor of φ^β specified under fully saturated conditions ($s^\beta = 1$). Finally, $\mathbf{K}^\beta$ is related to the intrinsic permeability $\mathbf{K}^S$ of the porous skeleton material through

$$\mathbf{K}^\beta = \frac{\gamma^{\beta R}}{\mu^{\beta R}} \mathbf{K}^S . \qquad (67)$$

Note that this equation can also be used to determine the Darcy permeability tensor $\mathbf{K}^\beta$ of various fluids from the intrinsic permeability $\mathbf{K}^S$ through the specific weights $\gamma^{\beta R}$ and the effective shear viscosities $\mu^{\beta R}$. In order to describe the deformation dependence of $\mathbf{K}^S$, it is assumed following Eipper [34] that

$$\mathbf{K}^S = \left(\frac{1 - n^S}{1 - n^S_{0S}} \right)^\pi \mathbf{K}^S_{0S} , \qquad (68)$$

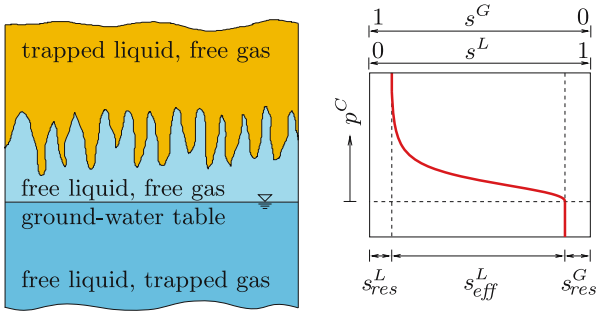

Fig. 2. Zones of partially saturated soil (left) and principle sketch of the capillary-pressure-saturation relation (right).

where $\mathbf{K}^S_{0S}$ is the intrinsic permeability tensor of the undeformed skeleton, and π is a material parameter governing the exponential function (68). If an initially isotropic solid is concerned, $\mathbf{K}^S_{0S}$ reduces to

$$\mathbf{K}^S_{0S} = K^S_{0S}\,\mathbf{I} \tag{69}$$

governed by a single initial intrinsic permeability coefficient K^S_{0S}. In analogy to (67), this coefficient is related to an initial Darcy permeability coefficient k^β_{0S} by

$$k^\beta_{0S} = \frac{\gamma^{\beta R}}{\mu^{\beta R}}\,K^S_{0S}. \tag{70}$$

Concerning partially saturated soil, three zones have to be distinguished, cf. Figure 2. In the zone beneath the ground-water table (saturated domain), most of the pore space is filled with the pore liquid, which is mobile and is governed by the Darcy permeability measured under fully saturated conditions. Nevertheless, there is a small amount of trapped pore gas in this zone with a residual saturation s^G_{res}. In a certain height above the ground-water table (empty domain), the pore gas is mobile, whereas a small amount of the pore liquid is trapped with the residual saturation s^L_{res}. In between these zones, there is the unsaturated or the partially saturated domain, respectively, where both fluids are mobile. The particular height of this domain depends on the suction properties of the soil material under study. In order to obtain a relation between the pore fluid mobilities through a relation between the liquid saturation and the capillary pressure, one usually proceeds from relations following Brooks and Corey [12] or van Genuchten [57]. In the present contribution, use is made of the van Genuchten model embedded in the general constitutive framework (60)–(62). Particularly, the model is given by

$$s^L_{\text{eff}}(p^C) = [\,1 + (\alpha_{\text{gen}}\,p^C)^{j_{\text{gen}}}\,]^{-h_{\text{gen}}}. \tag{71}$$

Therein, α_{gen}, j_{gen} and h_{gen} are material parameters, whereas the effective saturation function describing the area between the two residual saturations is given with respect to Finsterle [36], cf. Figure 3:

$$s^L_{\text{eff}} := \frac{s^L - s^L_{\text{res}}}{1 - s^L_{\text{res}} - s^G_{\text{res}}}. \tag{72}$$

In the van Genuchten model, the relative permeability functions are given by

$$\begin{aligned} \kappa^L_r &= (s^L_{\text{eff}})^{\epsilon_{\text{gen}}}\,\{1 - [1 - (s^L_{\text{eff}})^{1/h_{\text{gen}}}]^{h_{\text{gen}}}\}^2, \\ \kappa^G_r &= (1 - s^L_{\text{eff}})^{\gamma_{\text{gen}}}\,[1 - (s^L_{\text{eff}})^{1/h_{\text{gen}}}]^{2h_{\text{gen}}}, \end{aligned} \tag{73}$$

where ϵ_{gen} and γ_{gen} are additional parameters governing the hydraulic behaviour of the soil in the unsaturated domain, cf. Figure 3. If the effective saturation vanishes, κ^L_r is zero, and one obtains an immobile pore liquid. On the other hand, if the effective saturation is one, κ^L_r is one, and the pore liquid is fully mobile with the Darcy permeability under fully saturated conditions. Concerning the pore gas, equivalent statements hold. Inserting (65) into the quasi-static fluid momentum balances $(47)_2$ yields the Darcy-like equations

$$\begin{aligned} n^G\mathbf{w}_G &= -\frac{\mathbf{K}^G_r}{\gamma^{GR}}\,[\,\text{grad}\,p^{GR} - \rho^{GR}\,\mathbf{g}\,], \\ n^L\mathbf{w}_L &= -\frac{\mathbf{K}^L_r}{\gamma^{LR}}\Big[\,\text{grad}\,p^{LR} - \rho^{LR}\,\mathbf{g} \\ &\qquad - \frac{p^C}{n^L}(s^G\text{grad}\,n^L - s^L\text{grad}\,n^G)\Big], \end{aligned} \tag{74}$$

where $n^G\mathbf{w}_G$ and $n^G\mathbf{w}_G$ are the filter velocity of the pore gas and the pore liquid.

Finally, the effective density function of the pore gas is assumed to be governed by Boyle's ideal gas law

$$\rho^{GR} = \frac{p^{GR} + p_0}{\bar{R}^G\,\theta}. \tag{75}$$

Therein, $\bar{R}^G$ is the specific gas constant of the pore gas. Note that θ is constant ($\theta = \text{const.}$) due to the assumption of an overall isothermal problem.

The solid constituent. Following the geometrically linear approach of small strain elasto-plasticity, the solid strain tensor $\mathbf{E}_S$ is linearised to yield

$$\mathbf{E}_{Slin.} = \boldsymbol{\varepsilon}_S =: \tfrac{1}{2}\,[\,\text{grad}\,\mathbf{u}_S + (\text{grad}\,\mathbf{u}_S)^T\,]. \tag{76}$$

Furthermore, $\boldsymbol{\varepsilon}_S$ additively decomposed into an elastic and a plastic part:

$$\boldsymbol{\varepsilon}_S =: \boldsymbol{\varepsilon}_{Se} + \boldsymbol{\varepsilon}_{Sp}. \tag{77}$$

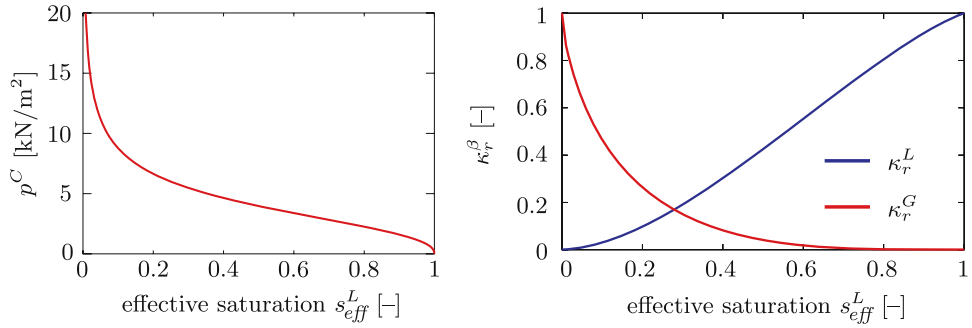

Fig. 3. Capillary-pressure-saturation relation (left) and relative permeability factors (right) after [57] with $\alpha_{\text{gen}} = 2 \cdot 10^{-4}$, $j_{gen} = 2.3$, $h_{\text{gen}} = 1.5$, $\epsilon_{\text{gen}} = 0.5$ and $\gamma_{\text{gen}} = 0.333$.

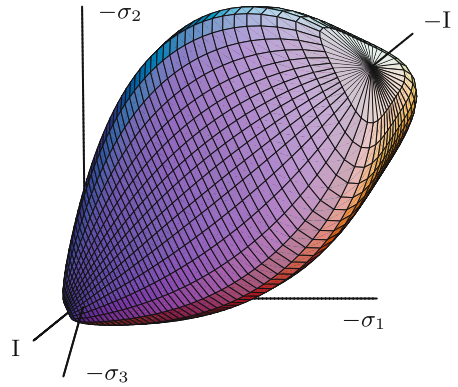

Fig. 4. Single-surface yield criterion for cohesive-frictional materials; σ_1, σ_2, σ_3: principal stresses of σ_E^S (tension positive).

Embedded in the general constitutive relations (60)–(62), the solid extra stress is governed by the generalised Hookean law

$$\sigma_E^S = \rho_{0S}^S \frac{\partial \psi^S}{\partial \varepsilon_{Se}} = 2\mu^S \varepsilon_{Se} + \lambda^S (\varepsilon_{Se} \cdot \mathbf{I})\mathbf{I}, \tag{78}$$

where μ^S and λ^S are the Lamé constants of the porous soil and σ_E^S is the solid extra stress under small strain conditions ($\sigma_E^S \approx \mathbf{T}_E^S$), where no difference between the Cauchy, the Kirchhoff, the Piola and the Piola-Kirchhoff stress must be made.

In order to describe the plastic or the viscoplastic material properties of the skeleton material, one has to consider a convenient yield function to bound the elastic domain. Following this, the single-surface yield criterion by Ehlers [16, 17] is applied, cf. Figure 4:

$$\begin{aligned} F &= \Phi^{1/2} + \beta \mathrm{I} + \epsilon \mathrm{I}^2 - \kappa = 0, \\ \Phi &= \mathrm{II}^D (1 + \gamma\vartheta)^m + \tfrac{1}{2}\alpha \mathrm{I}^2 + \delta^2 \mathrm{I}^4, \\ \vartheta &= \mathrm{III}^D / (\mathrm{II}^D)^{3/2}. \end{aligned} \tag{79}$$

In this yield function, which has been designed for cohesive-frictional materials, I, II^D and III^D are the first principal invariant of σ_E^S and the (negative) second and third principal invariants of the effective stress deviator $(\sigma_E^S)^D$. The material parameter sets

$$\mathscr{S}_h = \{\alpha, \beta, \delta, \epsilon, \kappa\}, \qquad \mathscr{S}_d = \{\gamma, m\} \tag{80}$$

govern the shape of the yield surface in the hydrostatic plane ($\mathscr{S}_h$) and in the deviatoric plane ($\mathscr{S}_d$). Proceeding either from the viscoplastic approach or from the perfect plasticity concept, the parameters included in $\mathscr{S}_h$ and in $\mathscr{S}_d$ are kept constant during the deformation process and can be computed from standard experimental data by use of an optimisation procedure [30,49,52].

Since the associated plasticity concept cannot be applied to frictional materials [45], an additional plastic potential [48]

$$G = \Gamma^{1/2} + \nu_2 \mathrm{I} + \epsilon \mathrm{I}^2 \text{ with } \Gamma = \nu_1 \mathrm{II}^D + \tfrac{1}{2}\alpha \mathrm{I}^2 + \delta^2 \mathrm{I}^4 \tag{81}$$

is considered, where ν_1 and ν_2 serve to relate the dilatation angle to experimental data. From the concept of the plastic potential, it is straight forward to obtain the evolution equation (flow rule) for the plastic strain ε_{Sp} via

$$(\varepsilon_{Sp})'_S = \Lambda^p \frac{\partial G}{\partial \sigma_E^S}, \tag{82}$$

where Λ^p is the plastic multiplier.

In the framework of viscoplasticity using the overstress concept of Perzyna-type [50], the plastic multiplier included in (82) is given by

$$\Lambda^p = \frac{1}{\eta} \left\langle \frac{F(\sigma_E^S)}{\sigma_0} \right\rangle^r. \tag{83}$$

Therein, $\langle \cdot \rangle$ are the Macaulay brackets, η is the relaxation time, σ_0 the reference stress, and r is the viscoplastic exponent. However, in the framework of elasto-plasticity, where the plastic strains are rate-independent, Λ^p has to be computed from the Kuhn-Tucker conditions

$$F \le 0, \quad \Lambda^p \ge 0, \quad \Lambda^p F = 0 \tag{84}$$

rather than from (83).

Weak forms and basic numerical setting. The numerical treatment of initial boundary-value problems of unsaturated soil described as a triphasic material is based on the weak formulations of the governing field equations together with discretisation methods in the space and time domains. As was mentioned above, the isothermal problem is basically governed by five independent fields: the solid displacement $\mathbf{u}_S$, the seepage velocities $\mathbf{w}_L$ and $\mathbf{w}_G$ and the effective fluid pressures p^{LR} and p^{GR}. However, under quasi-static conditions, Darcy-like relations (74) have been found to eliminate the seepage velocities by the effective fluid pressures. Consequently, the problem is finally governed by the variables $\mathbf{u}_S$, p^{LR} and p^{GR} corresponding, in the framework of the standard Galerkin procedure (Bubnov-Galerkin) to the balance relations (54).

Following these remarks, the overall momentum balance $(54)_1$ is multiplied by a test function $\delta\mathbf{u}_S$ and integrated over the domain Ω. Thus, one obtains

$$\int_\Omega [\operatorname{div}(\sigma_E^S - p\mathbf{I}) \cdot \delta\mathbf{u}_S + \rho\,\mathbf{g} \cdot \delta\mathbf{u}_S]\,\mathrm{d}v = 0\,, \tag{85}$$

where (63) and $\mathbf{T}_E^S \approx \sigma_E^S$ have been used. Integration by parts of the first term in (85) together with the Gaussian integral theorem finally yields

$$\int_\Omega (\sigma_E^S - p\mathbf{I}) \cdot \operatorname{grad}\delta\mathbf{u}_S\,\mathrm{d}v = \int_\Omega \rho\mathbf{g} \cdot \delta\mathbf{u}_S\,\mathrm{d}v + \int_{\Gamma_t} \bar{\mathbf{t}} \cdot \delta\mathbf{u}_S\,\mathrm{d}a. \tag{86}$$

Therein, $\bar{\mathbf{t}} = (\sigma_E^S - p\mathbf{I})\mathbf{n}$ is the total external load vector acting on the Neumann boundary Γ_t of the overall medium with the outward-oriented unit surface normal $\mathbf{n}$.

Analogously, multiplication of the pore-liquid volume balance $(54)_2$ with a test function δp^{LR}, integration over the domain Ω, integration by parts and application of the Gaussian integral theorem yields

$$\begin{aligned}&\int_\Omega [(n^L)'_S + n^L \operatorname{div}(\mathbf{u}_S)'_S]\delta p^{LR}\,\mathrm{d}v \\ &\quad - \int_\Omega n^L \mathbf{w}_L \cdot \operatorname{grad}\delta p^{LR}\,\mathrm{d}v = -\int_{\Gamma_v} \bar{v}^L \delta p^{LR}\,\mathrm{d}a,\end{aligned} \tag{87}$$

where $\bar{v}^L = n^L\mathbf{w}_L \cdot \mathbf{n}$ is the efflux of liquid volume through the Neumann boundary Γ_v. Applying the same procedure to the pore-gas mass balance, a multiplication of $(54)_3$ with a test function δp^{GR} leads to

$$\begin{aligned}&\int_\Omega [n^G(\rho^{GR})'_S + (n^G)'_S\rho^{GR} + n^G\rho^{GR}\operatorname{div}(\mathbf{u}_S)'_S] \\ &\qquad \times \delta p^{GR}\,\mathrm{d}v - \int_\Omega n^G\rho^{GR}\mathbf{w}_G \cdot \operatorname{grad}\delta p^{LR}\,\mathrm{d}v \\ &= -\int_{\Gamma_q} \bar{q}^G\,\delta p^{GR}\,\mathrm{d}a\,.\end{aligned} \tag{88}$$

Therein, $\bar{q}^G = n^G\rho^{GR}\mathbf{w}_G \cdot \mathbf{n}$ is the efflux of gaseous mass through the Neumann boundary Γ_q.

The constitutive setting of the problem and the weak forms given through (86)-(88) are sufficient to solve initial boundary-value problems in the framework of unsaturated soil mechanics.

5.3 Swelling media and active materials as a biphasic, four-component aggregate

In soil mechanics as well as in biomechanics and various other fields, swelling problems occur and have to be described on a computational basis. The phenomenon of swelling is triggered by the fact that negative electrical charges are fixed to the skeleton material such that the chemical equilibrium can change as a result of the composition of an external solution. To give an example for this behaviour, consider a soot-coloured hydrogel disc, cf. Figure 5, that is taken from a given bathing solution, where it was in chemical equilibrium, and put into another one with a lower concentration of both cations and anions. As a result, the chemical equilibrium in the disc is violated and can only be gathered again, when the disc absorbs a certain amount of liquid such that the internal and external solutions are again in a state of chemical equilibrium. It is furthermore seen from Figure 5 that swelling phenomena are often accompanied by large deformations of the solid skeleton.

To describe swelling processes, one has to consider a biphasic material of solid skeleton φ^S with adhering fixed charges φ^{fc} and a pore fluid φ^F understood as a mixture of a liquid solvent φ^L, e.g. water, and dissolved solutes, e.g. positive and negative ions φ^+ and φ^- of a salt such as the monovalent Na^+CL^-. Based on the balance equations $(37)_{1,2}$, the biphasic, four-component material under study is governed by the following mass and momentum balances:

$$\left.\begin{aligned}&(\rho^\alpha)'_\alpha + \rho^\alpha \operatorname{div}\mathbf{x}'_\alpha = 0\,, \\ &\mathbf{0} = \operatorname{div}\mathbf{T}^\alpha + \rho^\alpha\mathbf{b}^\alpha + \hat{\mathbf{p}}^\alpha\end{aligned}\right\} \quad \alpha = \{S, L, +, -\} \text{ and}$$
$$\varphi^F = \bigcup_{\beta=L,+,-} \varphi^\beta\,. \tag{89}$$

To obtain (89), the same assumptions as to obtain (47) have been used, namely, quasi-static processes at constant temperature and a general absence of phase transitions. Based

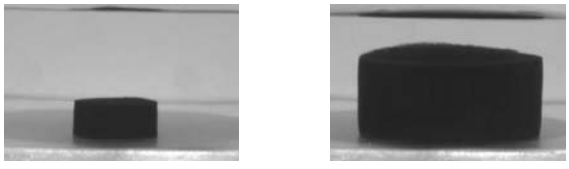

Fig. 5. Swelling experiment by Jacques Huyghe, TU Eindhoven (left: unswollen disc, right: finally swollen disc).

on the concept of material incompressibility ($\rho^{\alpha R} = \text{const.}$) of the porous solid including the fixed charges and the fluid components, liquid, cations and anions, the mass balances reduce to volume balances

$$(n^\alpha)'_\alpha + n^\alpha \operatorname{div} \mathbf{x}'_\alpha = 0\,. \tag{90}$$

Although the component densities $\rho^{\alpha R}$ are constant, the partial densities ρ^β_F (pore densities) of the fluid components as well as the effective pore-fluid density ρ^{FR} given by (8) and (9) can vary as a result of varying molar concentrations c^β_m in the pore-fluid mixture:

$$\rho^{FR} = \sum_{\beta=L,\gamma} \rho^\beta_F \quad \text{with} \quad \rho^\beta_F = c^\beta_m M^\beta_m \quad \text{and} \quad \gamma = \{+,-\}. \tag{91}$$

Since the molar masses M^β_m of the fluid components are constant, $(89)_1$ is rewritten to yield

$$\begin{aligned} &(n^F c^\beta_m)'_\beta + n^F c^\beta_m \operatorname{div} \mathbf{x}'_\beta = 0 \quad \text{or} \\ &n^F (c^\beta_m)'_\beta + c^\beta_m \operatorname{div} (\mathbf{u}_S)'_S + n^F c^\gamma_m \operatorname{div} \mathbf{w}_\beta \\ &\quad + c^\beta_m \operatorname{grad} n^F \cdot \mathbf{w}_\beta = 0\,, \end{aligned} \tag{92}$$

respectively. Proceeding from the fact that the fixed charges adhere to the skeleton material, thus sharing the skeleton motion, a volume balance for the fixed charges density is obtained as

$$(\rho^{fc})'_S + \rho^{fc} \operatorname{div} \mathbf{x}'_S = 0, \quad \text{where} \quad \rho^{fc} =: n^F c^{fc}_m M^{fc}_m. \tag{93}$$

Therein, c^{fc}_m and M^{fc}_m are the molar concentration and the molar mass of φ^{fc}. In analogy to obtaining (51) from (50), an integration of (93) yields

$$c^{fc}_m = n^F_{0S} c^{fc}_{m0S} (\det \mathbf{F}_S - n^S_{0S})^{-1}\,, \tag{94}$$

where c^{fc}_{m0S} and $n^F_{0S} = 1 - n^S_{0S}$ are the initial concentration and the initial fluid volume fraction (porosity) at $t = t_0$.

Proceeding from an isothermal four-component formulation of a biphasic material, quasi-static computational procedures are based on a basic set of seven primary variables given by the solid displacement $\mathbf{u}_S$, the pore fluid seepage velocity $\mathbf{w}_F$, the ionic seepage velocities $\mathbf{w}_+$ and $\mathbf{w}_-$, the hydraulic pore-fluid pressures $\mathscr{p}$ and the cation and anion concentrations c^+_m and c^-_m. Under quasi-static conditions, one obtains a coupling between $\mathbf{w}_F$ and $\mathscr{p}$ as well as between $\mathbf{w}_\gamma$ and c^γ_m resulting from the individual fluid momentum balances and the constitutive setting yielding Darcy-like and Nernst–Planck-like relations. Following this reduces the set of primary variables from seven to four: the solid displacement $\mathbf{u}_S$, the pore fluid pressure $\mathscr{p}$ and the ion concentrations c^γ_m. Thus, the corresponding set of governing equations is given by the overall momentum balance corresponding to $\mathbf{u}_S$, the fluid volume balance corresponding to $\mathscr{p}$ and the ion concentration balances corresponding to c^γ_m. Following this, one obtains in analogy to (54)

$$\begin{aligned} \mathbf{0} &= \operatorname{div} \mathbf{T} + \rho\, \mathbf{g}\,, \\ 0 &= (n^F)'_S + n^F \operatorname{div} (\mathbf{u}_S)'_S + \operatorname{div} (n^F\, \mathbf{w}_F) \\ &\quad + \frac{n^F}{\rho^{FR}} (\rho^{FR})'_F\,, \\ 0 &= n^F (c^\gamma_m)'_S + c^\gamma_m \operatorname{div} (\mathbf{u}_S)'_S + \operatorname{div} (n^F c^\gamma_m \mathbf{w}_\gamma)\,. \end{aligned} \tag{95}$$

Note that the ionic seepage and pore diffusion velocities are coupled through

$$\mathbf{w}_\gamma = \mathbf{d}_{\gamma F} + \mathbf{w}_F\,, \tag{96}$$

cf. $(15)_2$ and $(16)_2$. Furthermore, $(95)_1$ has been obtained in the same way as $(54)_1$, while $(95)_{2,3}$ represent the pore-fluid mass balance $(89)_1$ and the ion concentration balances $(92)_2$ both rearranged with respect to the skeleton motion.

Restrictions obtained from the entropy inequality. To close the model under consideration, constitutive equations are again required for the partial Cauchy stresses $\mathbf{T}^\alpha$ and the linear momentum productions $\hat{\mathbf{p}}^\beta$ of the fluid components. In addition, it will be shown that there is the need to formulate further constitutive equations for the chemical potentials and the osmotic pressure.

As was discussed in section 5.1, an evaluation of the overall entropy inequality

$$\begin{aligned} &\mathbf{T}^S \cdot \mathbf{L}_S - \rho^S (\psi^S)'_S \\ &\quad + \sum_\beta [\mathbf{T}^\beta \cdot \mathbf{L}_\beta - \rho^\beta (\psi^\beta)'_\beta - \hat{\mathbf{p}}^\beta \cdot \mathbf{w}_\beta] \geq 0 \end{aligned} \tag{97}$$

obtained from (45) for the swelling model under consideration imposes the necessary thermodynamical restrictions on the process. However, since the model includes a pore-fluid mixture instead of an immiscible combination of pore liquids and pore gases, the free energy functions of the fluid components will be formulated per fluid volume [9] instead of per constituent mass as in (97). Thus,

$$\begin{aligned} &\rho^\beta\, \psi^\beta = n^F (\rho^\beta_F \psi^\beta) =: n^F \Psi^\beta_F\,, \quad \text{where} \\ &\quad \Psi^\beta_F := \rho^\beta_F \psi^\beta. \end{aligned} \tag{98}$$

In addition, the pore-fluid free energy yields

$$\Psi^F_F := \sum_\beta \Psi^\beta_F\,. \tag{99}$$

Inserting (98) and (99) into (97), the entropy inequality transforms towards

$$\begin{aligned} &(\mathbf{T}^S - n^S \Psi^F_F \mathbf{I}) \cdot \mathbf{L}_S - \rho^S (\psi^S)'_S \\ &\quad + \sum_\beta [(\mathbf{T}^\beta - n^F \Psi^\beta_F \mathbf{I}) \cdot \mathbf{L}_\beta - n^F (\Psi^F_F)'_F \end{aligned}$$

$$
\begin{aligned}
&- \operatorname{grad} \Psi_F^\beta \cdot (n^F \mathbf{d}_{\beta F}) \\
&- (\hat{\mathbf{p}}^\beta + \Psi_F^\beta \operatorname{grad} n^F) \cdot \mathbf{w}_\beta] \geq 0. \qquad (100)
\end{aligned}
$$

Furthermore, the process is affected by two constraints, the saturation constraint and the electroneutrality constraint. These constraints read:

$$
\begin{aligned}
&\left(n^S + \sum_\beta n^\beta \right)'_S \\
&= -n^S \operatorname{div} \mathbf{x}'_S - \sum_\beta (n^\beta \operatorname{div} \mathbf{x}'_\beta + \operatorname{grad} n^\beta \cdot \mathbf{w}_\beta) = 0, \\
&\left(\rho_e^{fc} + \sum_\gamma \rho_e^\gamma \right)'_S \\
&= -\rho_e^{fc} \operatorname{div} \mathbf{x}'_S - \sum_\gamma (\rho_e^\gamma \operatorname{div} \mathbf{x}'_\gamma + \operatorname{grad} \rho_e^\gamma \cdot \mathbf{w}_\gamma) = 0. \qquad (101)
\end{aligned}
$$

To obtain the first constraint, the solid material time derivative of the saturation condition (4) has been taken, while to obtain the second constraint, the solid material time derivative has been applied to the the electroneutrality condition

$$
\rho_e = \rho_e^{fc} + \sum_\gamma \rho_e^\gamma = 0\,. \qquad (102)
$$

Therein, the densities of the volumetric electrical charges of the free moving ions φ^γ and the ions φ^{fc} adhering at the skeleton are given by

$$
\rho_e^\gamma := n^F z^\gamma c_m^\gamma F \quad \text{and} \quad \rho_e^{fc} := n^F z^{fc} c_m^{fc} F, \qquad (103)
$$

where z^γ are the valances of the ions, and F is the Faraday constant.

Multiplying the saturation constraint $(101)_1$ by the hydraulic pressure $\mathscr{P}$ and the electroneutrality constraint $(101)_2$ by the electrical potential $\mathscr{E}$, both acting as Lagrangean multipliers, the entropy inequality (100) yields after having been combined with these equations

$$
\begin{aligned}
&(\mathbf{T}_E^S - n^S \Psi_F^F \mathbf{I}) \cdot \mathbf{L}_S - \rho^S (\psi^S)'_S \\
&+ \sum_\beta [(\mathbf{T}_E^\beta - n^F \Psi_F^\beta \mathbf{I}) \cdot \mathbf{L}_\beta - n^F (\Psi_F^F)'_F \\
&- \operatorname{grad} \Psi_F^\beta \cdot (n^F \mathbf{d}_{\beta F}) \\
&- (\hat{\mathbf{p}}_E^\beta + \Psi_F^\beta \operatorname{grad} n^F) \cdot \mathbf{w}_\beta] \geq 0\,. \qquad (104)
\end{aligned}
$$

Therein, the electrical potential $\mathscr{E}$ occurs as a new field which is not matched by a governing equation yet. Concerning the further terms occurring in (104), the extra stresses $\mathbf{T}_E^S$ and $\mathbf{T}_E^\beta$ as well a the extra momentum productions $\hat{\mathbf{p}}_E^\beta$ with $\beta = \{L, \gamma\}$ are defined as

$$
\begin{aligned}
\mathbf{T}_E^S &= \mathbf{T}^S + n^S \mathscr{P} \mathbf{I} + \rho_e^{fc} \mathscr{E}\, \mathbf{I}, \\
\mathbf{T}_E^\gamma &= \mathbf{T}^\gamma + n^\gamma \mathscr{P} \mathbf{I} + \rho_e^\gamma\, \mathscr{E}\, \mathbf{I}, \\
\hat{\mathbf{p}}_E^\gamma &= \hat{\mathbf{p}}^\gamma - \mathscr{P} \operatorname{grad} n^\gamma - \mathscr{E} \operatorname{grad} \rho_e^\gamma, \\
\mathbf{T}_E^L &= \mathbf{T}^L + n^L \mathscr{P} \mathbf{I}, \qquad (105) \\
\hat{\mathbf{p}}_E^L &= \hat{\mathbf{p}}^L - \mathscr{P} \operatorname{grad} n^L\,.
\end{aligned}
$$

From the above relations, it is seen that the extra quantities and the total quantities are related to each other by the action of the incompressibility constraint $(101)_1$ multiplied by $\mathscr{P}$ and by the electroneutrality constraint $(101)_2$ multiplied by $\mathscr{E}$.

Combining (104) with the constitutive assumptions

$$
\psi^S = \psi^S(\mathbf{F}_S) \quad \text{and} \quad \Psi_F^\beta = \Psi_F^\beta(c_m^\beta) \qquad (106)
$$

yields with the aid of the standard evaluation procedure:

$$
\begin{aligned}
&\mathbf{T}_{E\,\text{mech.}}^S := \mathbf{T}_E^S + n^S \left(\sum_\beta c_m^\beta \frac{\partial \Psi_F^\beta}{\partial c_m^\beta} - \Psi_F^F \right) \mathbf{I}, \quad \text{where} \\
&\mathbf{T}_{E\,\text{mech.}}^S = \rho^S \frac{\partial \psi^S}{\mathbf{F}_S} \mathbf{F}_S^T, \\
&\mathbf{T}_{E\,\text{dis.}}^\beta := \mathbf{T}_E^\beta + n^F \left(c_m^\beta \frac{\partial \Psi_F^\beta}{\partial c_m^\beta} - \Psi_F^\beta \right) \mathbf{I}, \qquad (107) \\
&\hat{\mathbf{p}}_{E\,\text{dis.}}^\beta := \hat{\mathbf{p}}_E^\beta - \left(c_m^\beta \frac{\partial \Psi_F^\beta}{\partial c_m^\beta} - \Psi_F^\beta \right) \operatorname{grad} n^F\,.
\end{aligned}
$$

Therein, $\mathbf{T}_{E\,\text{mech.}}^S$ is the purely mechanical part of the solid extra stress, while $\mathbf{T}_{E\,\text{dis.}}^\beta$ and $\hat{\mathbf{p}}_{E\,\text{dis.}}^\beta$ are the frictional stresses and the drag and diffusion forces of φ^β. In addition to the results obtained with (107), it remains the dissipation inequality

$$
\mathscr{D} = -\sum_\beta \hat{\mathbf{p}}_{E\,\text{dis.}}^\beta \cdot \mathbf{w}_\beta \geq 0\,. \qquad (108)
$$

As has been stated in the previous section, a dimensional analysis has been used to neglect the frictional stresses $\mathbf{T}_{E\,\text{dis.}}^\beta$ in comparison with the momentum productions. As a result, the dissipation inequality is fulfilled with

$$
\begin{aligned}
\hat{\mathbf{p}}_{E\,\text{dis.}}^\gamma &= -\mathbf{S}^{\gamma S} \mathbf{w}_\gamma - \mathbf{S}^{L\gamma} (\mathbf{x}'_\gamma - \mathbf{x}'_L)\,, \\
\hat{\mathbf{p}}_{E\,\text{dis.}}^L &= -\mathbf{S}^{LS} \mathbf{w}_L - \sum_\gamma \mathbf{S}^{L\gamma} (\mathbf{x}'_L - \mathbf{x}'_\gamma)\,. \qquad (109)
\end{aligned}
$$

Therein,

$$
\mathbf{S}^{\beta S} = n^F \frac{n^\beta \mu^{\beta R}}{K^S} \mathbf{I} \quad \text{and} \quad \mathbf{S}^{L\gamma} = n^F \frac{n^L R\, \theta\, c_m^\gamma}{D^\gamma} \mathbf{I} \qquad (110)
$$

are the positive definite permeability and diffusion tensors under isotropic conditions, where D^γ is the ion diffusion coefficients of φ^γ and, as in the previous section, $\mu^{\beta R}$ is the effective shear viscosity of φ^β, and K^S is the intrinsic permeability of φ^S. Concerning the deformation dependence of K^S, cf. (67)–(70).

The fluid components. Based on the the assumption of vanishing frictional stresses $\mathbf{T}^{\beta}_{E\,\mathrm{dis.}}$, the extra stresses of the fluid components read

$$\mathbf{T}^{\beta}_{E} = -n^{F}\left(c^{\beta}_{m}\frac{\partial\Psi^{\beta}_{F}}{\partial c^{\beta}_{m}} - \Psi^{\beta}_{F}\right)\mathbf{I}$$

$$\text{yielding}\quad \mathbf{T}^{\beta}_{E} - n^{F}\Psi^{\beta}_{F}\,\mathbf{I} = n^{F}c^{\beta}_{m}\frac{\partial\Psi^{\beta}_{F}}{\partial c^{\beta}_{m}}\mathbf{I}. \tag{111}$$

From these relations, it is easily concluded that $(111)_2$ contains the molar chemical potential μ^{β}_{m} of φ^{β}, while $(111)_1$, as the "extra pressure" of φ^{β}, is the contribution π^{β} of φ^{β} to the overall osmotic pressure π. Thus,

$$\mu^{\beta}_{m} = \frac{\partial\Psi^{\beta}_{F}}{\partial c^{\beta}_{m}},\quad \pi^{\beta} = c^{\beta}_{m}\frac{\partial\Psi^{\beta}_{F}}{\partial c^{\beta}_{m}} - \Psi^{\beta}_{F} = c^{\beta}_{m}\mu^{\beta}_{m} - \Psi^{\beta}_{F}$$

$$\text{and}\quad \pi = \sum_{\beta}\pi^{\beta}. \tag{112}$$

Combining $(105)_{(1-3)}$, (107) and (111), one obtains the constituent partial stresses as

$$\begin{aligned}
\mathbf{T}^{S} &= -n^{S}(\mathscr{P}+\pi)\,\mathbf{I} \quad - \rho^{fc}_{e}\,\mathscr{E}\mathbf{I} + \mathbf{T}^{S}_{E\,\mathrm{mech.}},\\
\mathbf{T}^{\gamma} &= -n^{\gamma}\mathscr{P}\mathbf{I} - n^{F}\pi^{\gamma}\mathbf{I} \quad \rho^{\gamma}_{e}\mathscr{E}\mathbf{I},\\
\mathbf{T}^{L} &= -n^{L}\mathscr{P}\mathbf{I} - n^{F}\pi^{L}\mathbf{I},
\end{aligned} \tag{113}$$

where (99) has been used. Furthermore, one recovers the total momentum productions $(105)_{4,5}$ to yield

$$\begin{aligned}
\hat{\mathbf{p}}^{\gamma} &= \mathscr{P}\,\mathrm{grad}\;n^{\gamma} + \pi^{\gamma}\,\mathrm{grad}\;n^{F} + \mathscr{E}\,\mathrm{grad}\;\rho^{\gamma}_{e} + \hat{\mathbf{p}}^{\gamma}_{dis.},\\
\hat{\mathbf{p}}^{L} &= \mathscr{P}\,\mathrm{grad}\;n^{L} + \pi^{L}\,\mathrm{grad}\;n^{F} + \hat{\mathbf{p}}^{L}_{dis.}.
\end{aligned} \tag{114}$$

Finally, summing over the components of the pore-fluid mixture yields the overall fluid stress and the overall fluid momentum production, viz.:

$$\begin{aligned}
\mathbf{T}^{F} &= -n^{F}(\mathscr{P}+\pi)\,\mathbf{I} - \sum_{\gamma}\rho^{\gamma}_{e} \quad \mathscr{E}\,\mathbf{I},\\
\hat{\mathbf{p}}^{F} &= (\mathscr{P}+\pi)\,\mathrm{grad}\;n^{F} + \mathscr{E}\sum_{\gamma}\mathrm{grad}\;\rho^{\gamma}_{e} + \sum_{\beta}\hat{\mathbf{p}}^{\beta}_{E\,dis.}.
\end{aligned} \tag{115}$$

Ion diffusion and fluid flow. Proceeding from the standard assumption that the free energy of the fluid components can be given as

$$\Psi^{\beta}_{F} = c^{\beta}_{m}\mu^{\beta}_{0m} + c^{\beta}_{m}R\theta\,(\ln c^{\beta}_{m} - 1), \tag{116}$$

the chemical potentials and the osmotic pressure read

$$\mu^{\beta}_{m} = \mu^{\beta}_{0m} + R\theta\ln c^{\beta}_{m} \quad \text{and} \quad \pi = R\theta\,\textstyle\sum_{\beta}\,c^{\beta}_{m}. \tag{117}$$

Therein, μ^{β}_{0m} is known as the constant standard potential.

Inserting the partial ion stress $\mathbf{T}^{\gamma}$ from $(114)_2$ and the ion momentum production $\hat{\mathbf{p}}^{\gamma}$ from $(114)_1$ into the ion momentum balance $(89)_2$ yields

$$\begin{aligned}
\mathbf{0} = &-n^{\gamma}(\mathrm{grad}\;\mathscr{P} - \rho^{\gamma R}\mathbf{b}) - n^{F}\,\mathrm{grad}\;\pi^{\gamma}\\
&- \rho^{\gamma}_{e}\,\mathrm{grad}\;\mathscr{E} + \hat{\mathbf{p}}^{\gamma}_{E\,dis.}.
\end{aligned} \tag{118}$$

Since partial osmotic pressures cannot be measured, π^{γ} must be substituted by μ^{γ}_{m} with the aid of $(112)_2$. Thus, with the aid of $(106)_2$ and $(112)_1$, the ion momentum balance (118) yields

$$\begin{aligned}
\mathbf{0} = &-n^{\gamma}(\mathrm{grad}\;\mathscr{P} - \rho^{\gamma R}\mathbf{b}) - n^{F}\,c^{\gamma}_{m}\,\mathrm{grad}\;\mu^{\gamma}_{m}\\
&- \rho^{\gamma}_{e}\,\mathrm{grad}\;\mathscr{E} + \hat{\mathbf{p}}^{\gamma}_{E\,dis.}.
\end{aligned} \tag{119}$$

Proceeding from the assumption that the ion volume fraction n^{γ} is negligible compared to the liquid volume fraction n^{L} including

$$n^{\gamma} \ll n^{L} \quad \text{and} \quad n^{L} \approx n^{F}, \tag{120}$$

one obtains with the aid of (8)

$$\rho^{FR} \approx \rho^{L}_{F} \quad \text{with} \quad \sum_{\gamma}\rho^{\gamma}_{F} \approx 0 \quad \text{and} \quad \mathbf{x}'_{F} \approx \mathbf{x}'_{L}, \tag{121}$$

and (119) transforms towards the extended Nernst–Planck equation

$$n^{F}\mathbf{d}_{\gamma F} = -\frac{D^{\gamma}}{R\,\theta\,c^{\gamma}_{m}}\;(c^{\gamma}_{m}\,\mathrm{grad}\;\mu^{\gamma}_{m} + \rho^{\gamma}_{eF}\,\mathrm{grad}\;\mathscr{E}), \tag{122}$$

where $\mathbf{d}_{\gamma F} = \mathbf{x}'_{\gamma} - \mathbf{x}'_{F} \approx \mathbf{x}'_{\gamma} - \mathbf{x}'_{L}$ has been used. Furthermore, in analogy to $(8)_1$, $\rho^{\gamma}_{e} = n^{F}\rho^{\gamma}_{eF}$. In order to obtain (122) describing the ion diffusion process from (119), the first term on the rhs of (119), the drag term, has been neglected with respect to $(121)_1$. Furthermore, $\hat{\mathbf{p}}^{\gamma}_{E\,dis.}$ from (109) and (110) has been simplified with the same argument as before by dropping $\mathbf{S}^{\gamma S}$, cf. $(110)_1$. Expressing the chemical potentials μ^{γ}_{m} by the concentrations c^{γ}_{m} yields the final version of the diffusion equation (122), viz.:

$$n^{F}\mathbf{d}_{\gamma F} = -\frac{D^{\gamma}}{R\,\theta\,c^{\gamma}_{m}}\;(R\,\theta\,\mathrm{grad}\;c^{\gamma}_{m} + \rho^{\gamma}_{eF}\,\mathrm{grad}\;\mathscr{E}). \tag{123}$$

Therein, (117) together with the assumption of isothermal processes has been used.

Inserting the fluid stress and the fluid momentum production given by (115) into the fluid momentum balance obtained by summing $(89)_2$ over $\beta = \{L,+,-\}$ yields

$$\begin{aligned}
\mathbf{0} = -n^{F}&\left[\mathrm{grad}\;(\mathscr{P}+\pi) - \rho^{FR}\mathbf{b} - \sum_{\gamma}\rho^{\gamma}_{eF}\,\mathrm{grad}\;\mathscr{E}\right]\\
&+ \hat{\mathbf{p}}^{F}_{E\,\mathrm{dis.}}.
\end{aligned} \tag{124}$$

Therein, $\hat{\mathbf{p}}^F_{E\,\text{dis.}}$ is obtained from (109), (110) and $(121)_1$ as

$$\hat{\mathbf{p}}^F_{E\,\text{dis.}} = \hat{\mathbf{p}}^L_{E\,\text{dis.}} + \sum_\gamma \hat{\mathbf{p}}^\gamma_{E\,\text{dis.}} = -(n^F)^2\,\frac{\mu^{FR}}{K^S}\,\mathbf{w}_F. \tag{125}$$

Combining (124) and (125), one recovers the extended Darcy equation

$$n^F\,\mathbf{w}_F = -\frac{K^S}{\mu^{FR}}\left[\operatorname{grad}\,(\mathscr{P}+\pi) - \rho^{FR}\mathbf{b} - \sum_\gamma \rho^\gamma_{eF}\,\operatorname{grad}\,\mathscr{E}\right] \tag{126}$$

governing the fluid flow.

Electrical potential. The electrical potential $\mathscr{E}$ entering the process through the entropy inequality (104) together with the electroneutrality constraint $(101)_2$ reveals that there is no matching governing equation. Thus, this additional equation must be found and added to the process. To overcome this situation, use is made of the Poisson equation of the electrical potential of electrostatics yielding

$$\operatorname{div}\operatorname{grad}\,\mathscr{E} = -\frac{1}{\epsilon^F}\,\rho_e, \tag{127}$$

where $\operatorname{div}\operatorname{grad}\,(\cdot) =: \Delta\,(\cdot)$ is the Laplace operator, ϵ^F the constant electric fluid permittivity, while the density ρ_e of the electrical charges is given through (102) and (103). In contrast to the electroneutrality condition (102) stating $\rho_e = 0$, ρ_e is usually obtained from the Gaussian law

$$\operatorname{div}\mathbf{d}_e = \rho_e, \tag{128}$$

where $\mathbf{d}_e$ is the electric displacement obtained from the electrical field $\mathbf{e}$ via

$$\mathbf{d}_e = \epsilon^F\,\mathbf{e} \quad \text{with} \quad \mathbf{e} = -\operatorname{grad}\,\mathscr{E}. \tag{129}$$

Combining (127) with (103) finally yields

$$\operatorname{div}\operatorname{grad}\,\mathscr{E} = -\frac{n^F\,F}{\epsilon^F}\left(\sum_\gamma z^\gamma c^\gamma_m + z^{fc}c^{fc}_m\right). \tag{130}$$

This equation will be used in the numerical setting to match $\mathscr{E}$.

The solid skeleton. As was mentioned at the beginning of this subsection, swelling phenomena are usually combined with large solid deformations, cf. Figure 5. Following this results in the fact that a non-linear elasticity law is needed to describe the elastic solid deformations. Following Ehlers and Eipper [20], a combination of the Neo-Hookean law with a non-linear volumetric deformation yields by use of $(107)_1$

$$\mathbf{T}^S_{E\,\text{mech.}} = \rho^S\frac{\partial\psi^S}{\mathbf{F}_S}\,\mathbf{F}^T_S = (\det\mathbf{F}_S)^{-1}\Big[2\,\mu^S\,\mathbf{K}_S + \lambda^S\,(1-n^S_{0S})^2 \left(\frac{J_S}{1-n^S_{0S}} - \frac{J_S}{J_S-n^S_{0S}}\right)\mathbf{I}\Big], \tag{131}$$

where μ^S and λ^S, as in Subsection 5.2, are the Lamé constants. Concerning the description of finite volumetric deformations of a materially incompressible solid skeleton, recall that the property of material incompressibility ($\rho^{SR} = \text{const.}$) does not include total incompressibility ($\rho^S = \text{const.}$), since ρ^S can still change through n^S. As a result, the volumetric deformation included in (131) is only due to variations of the pore space, such as those initiated by swelling processes, and is not due to volumetric changes of the matrix material itself.

Weak forms and basic numerical setting. As was discussed before, the numerical treatment of initial boundary-value problems is based on the weak formulations of the governing field equations together with discretisation methods in the space and time domains. Concerning swelling media described as a biphasic, four-component material of a swellable solid skeleton φ^S including the fixed charges φ^{fc} and the pore fluid φ^F consisting of the liquid solvent φ^L and the cations φ^+ and anions φ^-, the isothermal problem under consideration is basically governed by eight independent fields: the solid displacement $\mathbf{u}_S$, the seepage and diffusion velocities $\mathbf{w}_F$, $\mathbf{d}_{+F}$ and $\mathbf{d}_{-F}$, the hydraulic pressure $\mathscr{P}$ as well as the ion concentrations c^+_m and c^-_m. In addition, the electrical potential $\mathscr{E}$ has to be considered. However, under quasi-static conditions, Nernst–Planck-like and Darcy-like relations, cf. (123) and (126), have been found to eliminate the seepage and diffusion velocities by the effective hydraulic pressure $\mathscr{P}$ and the ion concentrations c^γ_m. Thus, the remaining set of five independent fields must be matched by a corresponding set of five governing equations given through (95) by the overall momentum balance corresponding to $\mathbf{u}_S$, the fluid volume balance corresponding to $\mathscr{P}$ and the ion concentration balances corresponding to c^γ_m. In addition, the Poisson equation (130) is considered corresponding to $\mathscr{E}$.

In analogy to (85)-(88), one obtains the weak forms of the governing equations in the framework of the standard Galerkin procedure. In particular, the overall momentum balance $(95)_1$ is multiplied by a test function $\delta\mathbf{u}_S$ and integrated over the domain Ω. Integration by parts together with the Gaussian integral theorem yields the following result in the same way as to obtain (86) from (85):

$$\int_\Omega [\mathbf{T}^S_{E\,\text{mech.}} - (\mathscr{P}+\pi)\,\mathbf{I}]\cdot\operatorname{grad}\,\delta\mathbf{u}_S\,\mathrm{d}v = \int_\Omega \rho\,\mathbf{g}\cdot\delta\mathbf{u}_S\,\mathrm{d}v + \int_{\Gamma_t}\bar{\mathbf{t}}\cdot\delta\mathbf{u}_S\,\mathrm{d}a. \tag{132}$$

Therein, as in the previous section, $\bar{\mathbf{t}} = [\mathbf{T}^S_{E\,\text{mech.}} - (\mathscr{P} + \pi)\mathbf{I}]\,\mathbf{n}$ is the external load vector acting on the Neumann boundary Γ_t of the overall aggregate.

Proceeding from the assumption $\rho^{FR} \approx \rho^L_F$ resulting from $n^\gamma \ll n^L$, cf. (121), $(\rho^{FR})'_F$ vanishes and the fluid volume balance $(95)_2$ reduces to

$$\operatorname{div}\left[(\mathbf{u}_S)'_S + n^F\,\mathbf{w}_F\right] = 0, \tag{133}$$

where (90) with $\alpha = S$ has been used. Multiplying (133) by $\delta\mathscr{P}$ and using the same procedure as before results in

$$\begin{aligned}&\int_\Omega n^F\,\mathbf{w}_F \cdot \operatorname{grad}\,\delta\mathscr{P}\,\mathrm{d}v - \int_\Omega \operatorname{div}(\mathbf{u}_S)'_S\,\delta\mathscr{P}\,\mathrm{d}v\\ &\quad= \int_{\Gamma_v} \bar{v}^F\,\delta\mathscr{P}\,\mathrm{d}a.\end{aligned} \tag{134}$$

Therein, $\bar{v}^F = n^F\,\mathbf{w}_F \cdot \mathbf{n}$ is the efflux of fluid volume through the Neumann boundary Γ_v.

In a next step, the ion concentration balances $(95)_2$ have to be considered. After having multiplied these equations by δc^γ_m, one obtains in analogy to the above procedure

$$\begin{aligned}&\int_\Omega n^F\,c^\gamma_m\,(\mathbf{d}_{\gamma F} + \mathbf{w}_F)\cdot\operatorname{grad}\,\delta c^\gamma_m\,\mathrm{d}v\\ &\quad- \int_\Omega \left[n^F\,(c^\gamma_m)'_S + c^\gamma_m \operatorname{div}(\mathbf{u}_S)'_S\right]\delta c^\gamma_m\,\mathrm{d}v\\ &\quad= \int_{\Gamma_{J^\gamma}} \bar{j}^\gamma\,\delta c^\gamma_m\,\mathrm{d}a.\end{aligned} \tag{135}$$

Therein, with the aid (96), $\bar{j}^\gamma = n^F\,c^\gamma_m\,\mathbf{w}_\gamma \cdot \mathbf{n}$ is the ionic efflux through the Neumann boundary Γ_{J^γ}.

Finally, multiplying the Poisson equation (130) by $\delta\mathscr{E}$ and applying the same procedure as before results in

$$\begin{aligned}&\int_\Omega \operatorname{grad}\,\mathscr{E}\cdot\operatorname{grad}\,\delta\mathscr{E}\,\mathrm{d}v\\ &\quad- \int_\Omega \frac{n^F F}{\epsilon^F}\left(\sum_\gamma z^\gamma c^\gamma_m + z^{fc} c^{fc}_m\right)\delta\mathscr{E}\,\mathrm{d}v\\ &\quad= -\int_{\Gamma_e} \bar{e}\,\delta\mathscr{E}\,\mathrm{d}a,\end{aligned} \tag{136}$$

where $\bar{e} = \mathbf{e}\cdot\mathbf{n}$ is the electrical field across the Neumann boundary Γ_e.

The constitutive setting of the problem and the weak forms given through (132)–(136) are sufficient to solve initial boundary-value problems in the framework of swelling media.

6 Numerical examples

6.1 Preliminary remarks

The following numerical examples can only present some showcases exhibiting the behaviour of both unsaturated soil and electro-chemically-driven swelling media. In any case, the computational results of the initial boundary-value problems presented in this Section are computed by use of the Finite Element Analysis (FEA) satisfying the necessary stabilisation criteria.

Based on the weak forms (86)–(88) for partially saturated soil or on (132)–(136) for swelling media, the numerical scheme generally proceeds from a spatial discretisation (semi-discretisation with respect to the space variable $\mathbf{x}$) of the field equations by use of mixed finite elements (Taylor-Hood elements) satisfying the Ladyzhenskaya-Babuška-Brezzi (LBB) condition combined with a finite difference scheme in the time domain. In both regimes, the spatial and the temporal one, adaptive computations can be applied and can furthermore be combined with parallel computational strategies. Concerning further implementary and computational details, the interested reader is basically referred to the work by Lewis and Schrefler [46] or by Borja [8], if unsaturated soil mechanics is concerned, or to Chen *et al* [13], Frijns *et al* [37], Huyghe and Janssen [41], Huyhge *et al* [42], Kaasschieter *et al* [43], Loret *et al* [47], Samson *et al* [51] and Wallmersperger [58], if swelling media are concerned, and to the work by the group of the author [1, 24–28, 31, 32, 39, 44, 59–61] and references therein.

6.2 Unsaturated soil

Based on the weak forms (86)–(88), the numerical scheme governing the spatial domain is based on extended Taylor-Hood elements with quadratic shape functions for the solid displacement $\mathbf{u}_S$ and linear shape functions for the effective fluid pressures p^{LR} and p^{GR}. In contrast to the computation of the external variables $\mathbf{u}_S$, p^{LR} and p^{GR}, the plastic strains ε_{Sp} and the plastic multiplier Λ^p determined by (82) and (83) act as internal variables and must thus be computed, in the sense of the collocation method, at the integration points of the numerical quadrature, cf. Ellsiepen [35] for details.

The following numerical example concerns a 2-dimensional (2-d), plane-strain description of the liquid flow through an embankment with elasto-plastic soil properties, cf. Figure 6. In particular, the embankment has a height of 10 m and a slope gradient on both sides of $s = 1/3$.

Furthermore, the ground level is assumed to be more or less impermeable governed by an intrinsic permeability of $K^S_{0S} = 10^{-15}\,\mathrm{m}^2$ implying a liquid Darcy permeability of $k^L_{0S} = 10^{-8}\,\mathrm{m/s}$. The embankment itself proceeds from the

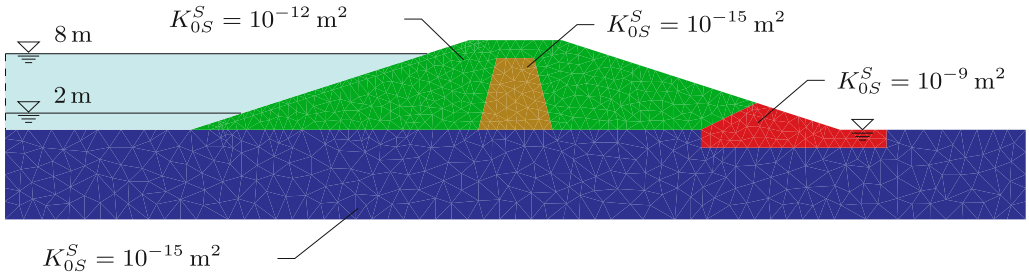

Fig. 6. Embankment with a central seal unit.

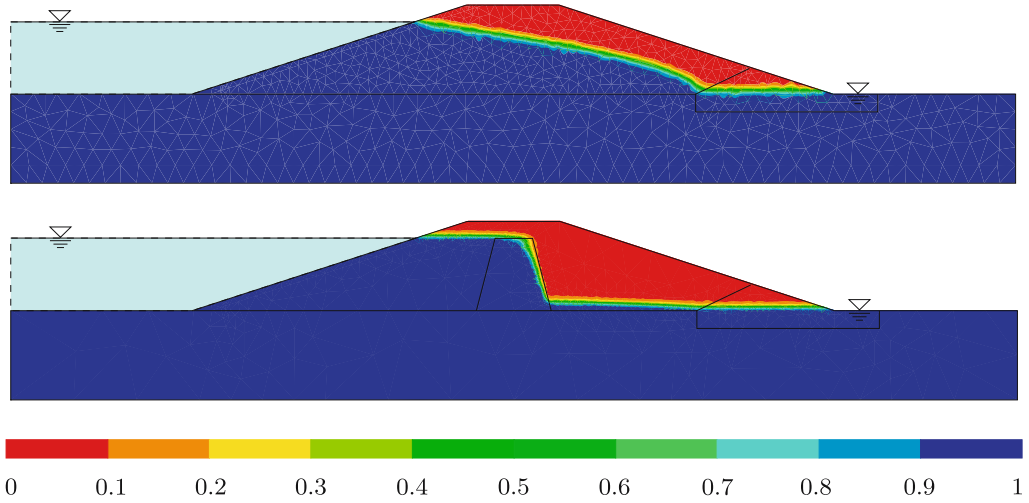

Fig. 7. Pore-liquid saturation in the stationary state: embankment without a seal unit (top), embankment with a central seal unit (bottom).

values of $K_{0S}^S = 10^{-12}\,\mathrm{m}^2$ and $k_{0S}^L = 10^{-5}\,\mathrm{m/s}$, whereas the filter at the right-hand side of the structure is assumed to be governed by $K_{0S}^S = 10^{-9}\,\mathrm{m}^2$ and $k_{0S}^L = 10^{-2}\,\mathrm{m/s}$. In order to exhibit the differences between typical embankment constructions, the embankment problem is discussed twicely, namely, with and without a central seal unit governed by the same permeability properties like the ground level.

Based on the triphasic formulation, it is assumed that a water table of 2 m height at the left side (water side) of the embankment is rapidly increased towards 8 m, cf. Figure 6. As a result, water streams into the embankment and finally reaches a stationary state, cf. Figure 7, where three different domains can be distinguished. These are the fully water-saturated domain (blue) with only a few parts of immobile air, the air-saturated domain (red) with only a few parts of immobile water and the unsaturated domain in between (yellow) with both mobile water and mobile air. Because of the different embankment constructions, the stationary state is reached after very different times. If there is no seal unit, the fluid flow in the dam reaches the stationary state 57 days after the increase of the water table. In contrast, as a result of the seal unit, the sealed dam only reaches the stationary state after 6.3 years, which makes a big difference concerning the safety of the overall construction. In particular, it is easily realised that the seal unit prevents the right part of the embankment (air side) from an increasing water table. As a result of not being under buoyancy conditions, the stability of the air side of the embankment is significantly improved.

The investigation of embankment stability problems is a crucial issue and has to be investigated very carefully. In particular, instabilities are usually initiated by the localisation of plastic deformations in narrow bands, the so-called shear bands, driven by gravitational forces and local saturation values. Furthermore, the onset of localisations can appear on both sides of the embankment, the water side as well as the air side. However, both a moderate embankment slope angle and the existence of a filter unit at the air side help to prevent the embankment construction from stability problems. Concerning the construction and the geometry of the example computed above, no shear band development could be found. Nevertheless, there are geometries and technical layouts of embankments which are very sensitive to stability phenomena. To support this statement, a further boundary-value problem is presented, where the construction, on the one hand, has neither been provided with a seal unit nor with

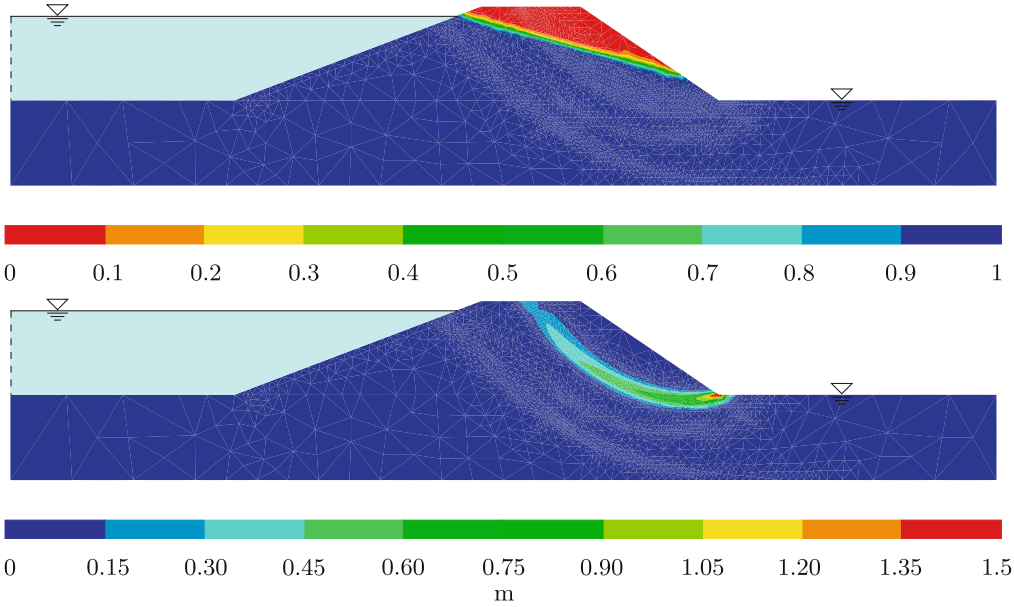

Fig. 8. Saturation of the pore liquid (top) and localisation of the accumulated plastic strains $[10^{-1}]$ (bottom).

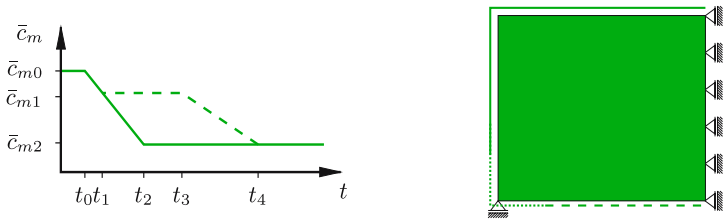

Fig. 9. Chemical loading and geometry of a 2-d free swelling simulation. The solid and the dashed concentration curves on the left side belong to the respective boundaries on the right side. The dotted line at the bottom's left corner of the right-hand picture denotes the interval with the transition zone from the value of the solid concentration curve to the dashed one.

a filter at the air side and, on the other hand, the slope at the air side is much steeper than before.

In this regard, it is assumed that the slope gradient at the water side keeps its original value of $s = 1/3$, whereas, at the air side, there is a stronger inclination given by an angle of 35°. As a result of the water table at the left side of the embankment in combination with the missing filter unit, water is leaking from the embankment at the air side through the slope, cf. Figure 8, thus effecting major parts of the embankment by buoyancy forces. As a consequence, one observes the onset of a shear band at the air side, starting at the kink between the slope and the ground level. Note in passing that this situation is very typical to appear in case of natural hazards initiated, e.g., by extremely heavy rainfall events and comparable situations. If shear banding occurs, the embankment needs to be prevented from destruction. For example, this can be done by loading the air side of the embankment by additional weights given, e.g., by sandbags.

Finally, it should be mentioned with respect to the well-known ill-posedness of the localisation problem that a non-regularised space-adaptive computation would reveal a shear band thickness shrinking with the element size. In order to overcome this unphysical behaviour, a regularisation of the problem is mandatory and has been applied to the present computations by the consideration of a slightly modified solid behaviour by adding viscoplastic effects, cf. (83). Further regularisation strategies are possible and have been commented in the literature.

6.3 Swelling media and electro-active gels

Swelling media. Based on the weak forms (132)–(136), the numerical scheme governing swelling media is again based on extended Taylor-Hood elements with quadratic shape functions for the solid displacement $\mathbf{u}_S$ and linear shape functions for hydraulic fluid pressure $\mathscr{P}$, the ion concentrations c_m^+ and c_m^- and the electrical potential $\mathscr{E}$.

The following numerical example concerns a 2-d plane-strain simulation of the swelling experiment carried out

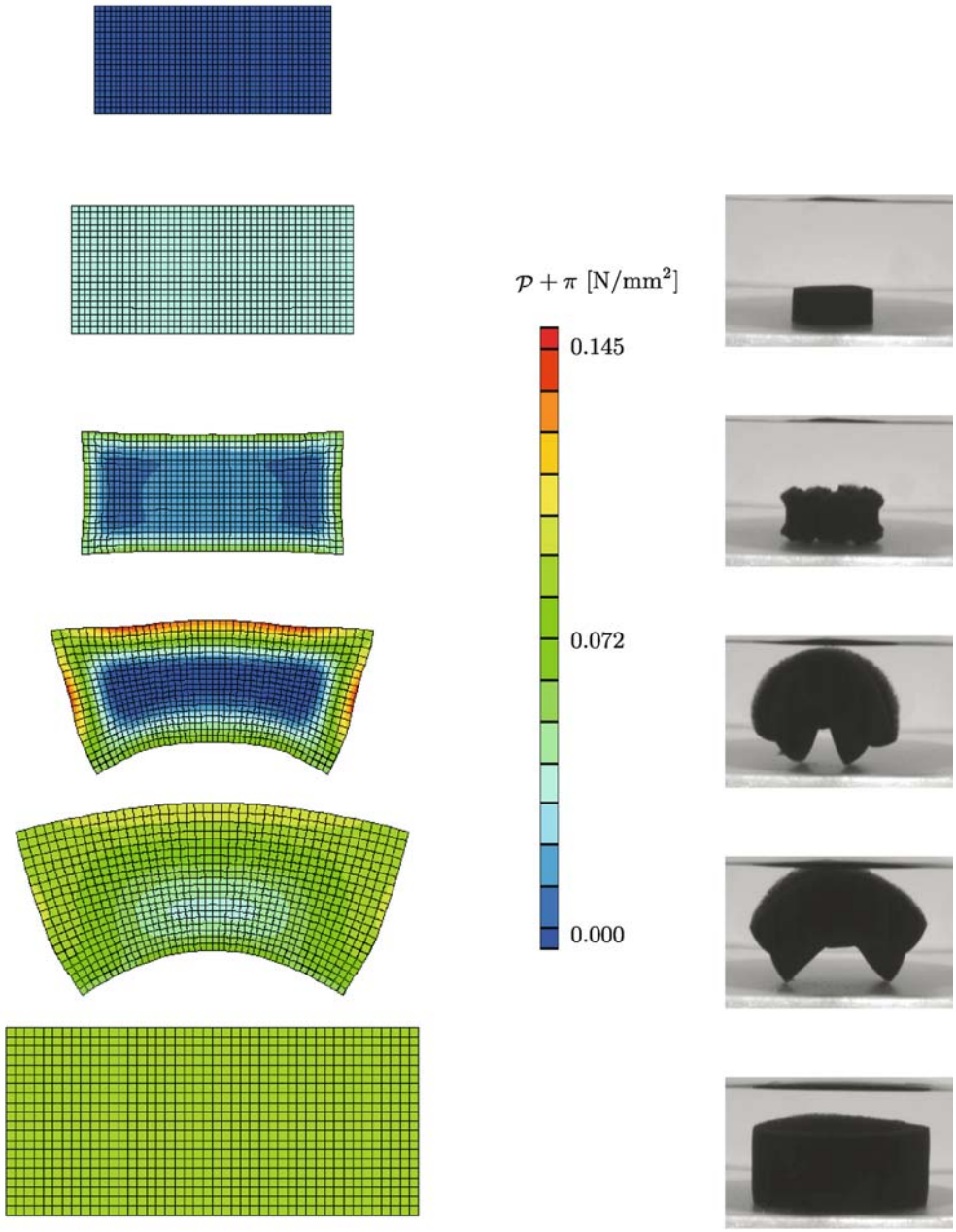

Fig. 10. Qualitative comparison between the numerical simulation and the experiment with a soot-coloured hydrogel disc carried out by the group of Jacques Huyghe. The most upper geometry on the left is the stress-free and non-swollen reference configuration. Beneath, there is the pre-swollen initial state. The following contour plots show the deformation and the overall pressure (hydraulic and osmotic) up to the final equilibrium state.

by the group of Jacques Huyghe in Eindhoven (The Netherlands), cf. Figure 5. To simulate this experiment, a rectangular cross section is discretised under symmetry conditions. During the computation, the chemically uncharged hydrogel is firstly equilibrated in a bathing solution with the initial external concentration $\bar{c}_{m0}$. This is necessary in order to transform the hydrogel from a fictitious non-loaded reference configuration in the sense of a natural state at $t = t_0$ towards a pre-swollen initial configuration. Note in passing that there is no uncharged configuration in any real experiment, since swelling materials are always somehow in a swollen state. In the fictitious non-loaded reference configuration, there is neither a solid stress ($\mathbf{T}^S_{E\,mech.0S} = \mathbf{0}$) nor an osmotic pressure ($\pi_0 = 0$). To avoid numerical problems during initial loading, the initial osmotic pressure is applied slowly by increasing the referential concentration of the fixed charges from 0 to the prescribed value c^{fc}_{m0S} over time.

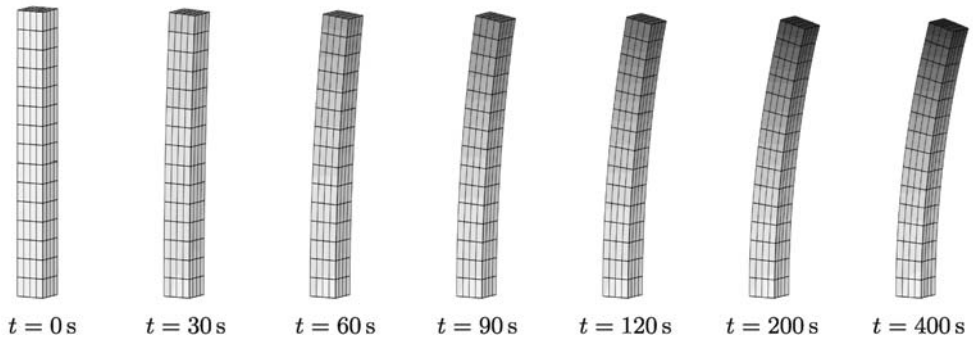

Fig. 11. Deformation behaviour of the cantilever made of an EAP. The largest deflection of 1.3 mm is displayed in black, while white represents a deflection of 0 mm.

After a certain time of computation, an equilibrium state is reached defined as the "initial configuration" at which the initial osmotic pressure π_0^*, the initial concentration c_{m0}^* and the initial purely mechanical solid extra stress $\mathbf{T}_{E\,mech.\,0S}^{S*}$ fits the volumetric deformation $(\det \mathbf{F}_S)_{0S}^*$ through the balance equations and the constitutive setting.

Concerning the numerical simulation prior to the actual swelling process, cf. Figure 9, the specimen is equilibrated for a period of $t_0 = 7000\,\mathrm{s}$ in a $\bar{c}_{m0} = 4.1$ molar NaCl solution, where c_{m0S}^{fc} is increased from 0 to 0.8 meq/l within the first 4000 s. After an equilibrium state is obtained, the initial configuration is reached, and the hydrogel is placed in another NaCl solution. There, the external salt concentration is decreased at all boundaries from $\bar{c}_{m0} = 4.1\,\mathrm{mol/l}$ to $\bar{c}_{m1} = 2.7\,\mathrm{mol/l}$ until $t_1 = 7080\,\mathrm{s}$. Thereafter, only the boundaries denoted by the solid line are exposed to the solution. Here, the concentration is further decreased to $\bar{c}_{m2} = 0.3\,\mathrm{mol/l}$ until $t_2 = 7220\,\mathrm{s}$, while the concentration at the bottom is kept constant. At $t_3 = 8000\,\mathrm{s}$, the bottom of the hydrogel gets in contact with the bathing solution as well. Therefore, $\bar{c}_{m1}$ is decreased here to $\bar{c}_{m2} = 0.3\,\mathrm{mol/l}$ until $t_4 = 10000\,\mathrm{s}$.

In Figure 10, the simulation results on the left-hand side are compared to the experiment on the right-hand side. Besides the comparison of the deformation, the contour plots show the development of the overall fluid pressure within the material. The left top picture shows the artificial stress-free reference configuration at $t = 0\,\mathrm{s}$, where there is no deformation and no osmotic pressure. Beneath, one can see the computed initial configuration ($t_0 = 7000\,\mathrm{s}$) after having increased c_{0S}^{fc} from 0 to its full amount and after having reached chemical equilibrium. This is a swollen state, i. e., there is an osmotic pressure and a deformation. The third line shows the phase of the negative osmosis ($t = 7107\,\mathrm{s}$), during which the hydrogel shrinks initially in its inner region. Note in passing that this effect results from the state of chemical non-equilibrium at the domain boundary yielding an influx of liquid both from the bathing solution through the domain boundary and from the inner part of the specimen to outer parts. Thereafter, the state with the greatest bending is shown ($t = 7224\,\mathrm{s}$). The subsequent pictures present how the final equilibrium state is reached ($t = 7650\,\mathrm{s}$ and $t = 11000\,\mathrm{s}$). At the end of the simulation process, the cross-sectional area of the specimen is approximately 2.2 times larger than the area of the computed initial state.

Electro-active polymers. In order to simulate the response of an electro-active polymer (EAP) to an applied electrical field, the final example concerns a 3-d hydrogel cantilever (1 mm by 1 mm by 10 mm) which is exposed to a voltage of 0.8 V. Following this, the displacements at the bottom surface are disabled such that the applied voltage leads to a bending of the EAP. In particular, the electrical potential $\bar{\varphi}$ included in the boundary term $\bar{e}$, cf. (136), is linearly applied within 4 s, thereby increasing the left side from 0 V to 0.4 V, while decreasing the voltage from 0 V to −0.4 V on the opposite (right) side. Moreover, since the EAP is placed in a bathing solution, the molar concentration $\bar{c}_m^\gamma = 1.0\,\mathrm{mol/l}$ of both ions is kept constant at all boundaries. Figure 11 illustrates the deformation behaviour of the cantilever at different time steps, whereas the shading indicates the deflection of the cantilever.

7 Conclusion

It was the goal of the present article to range from basic continuum-mechanical approaches of the Theory of Mixture (TM) and the Theory of Porous Media (TPM) via the constitutive modelling of sophisticated multiphasic and multiphysical problems to computational simulations of challenging initial boundary-value problems. However, apart from the general setting of continuum-mechanically coupled problems, only two instructive models could be discussed in detail, namely, the unsaturated soil problem treated as a triphasic aggregate of an elasto-plastic soil skeleton saturated by an arbitrary combination of a pore liquid (water) and a pore gas (air) and a biphasic, four-component material describing swelling media and electro-active polymers. While

the solid deformations of the first example have been considered geometrically linear, swelling media generally exhibit finite deformations. In the numerical range, both problems have been embedded in the Finite Element Analysis, thus yielding sound numerical results. In particular, the numerical results of the unsaturated soil example have been taken from Ehlers, Graf and Ammann [27], whereas the results of the swelling media example have been taken from Ehlers and Acartürk [31] and those of the electro-active polymer from Ehlers and Karajan [33]. Material parameters which have not been included in this article, can also be found in these articles. The interested reader who wants to see further computational examples from the broad field of mechanical, civil, environmental and biomechanical engineering is referred to the relevant literature or to the work by the author and his group, cf. http://mechbau.uni-stuttgart. de/ls2.

References

1. Acartürk A., Simulation of Charged Hydrated Porous Materials. Dissertation, Report No. II-18 of the Institute of Applied Mechanics (CE), University of Stuttgart (2009)
2. Bishop A.W., The effective stress principle. *Teknisk Ukeblad*, **39**, 859–863 (1959)
3. de Boer R., Highlights in the historical development of porous media theory: Toward a consistent macroscopic theory. *Applied Mechanics Review*, **49**, 201–262 (1996)
4. de Boer R., Theory of Porous Media, Springer, Berlin (2000)
5. de Boer R. and Ehlers W., Theorie der Mehrkomponentenkontinua mit Anwendung auf bodenmechanische Probleme. Forschungsberichte aus dem Fachbereich Bauwesen 40, Universität Essen (1986)
6. de Boer R. and Ehlers W., Uplift, friction and capillarity – three fundamental effects for liquid-saturated porous media, *International Journal of Solids Structures*, **26**, 43–57 (1990)
7. de Boer R. and Ehlers W., The development of the concept of effective stresses, *Acta Mechanica*, **83**, 77–92 (1990)
8. Borja R., Bifurcation of elastoplastic solids to shear band mode at finite strain, *Computer Methods in Applied Mechanics and Engineering*, **191**, 5287–5314 (2002)
9. Bowen R.M., Theory of mixtures, In: Continuum Physics, (Ed.) Eringen A.C., Vol. III, pp. 1–127. Academic Press, New York (1976)
10. Bowen R.M., Incompressible porous media models by use of the theory of mixtures, *International Journal of Engineering Science*, **18**, 1129–1148 (1980)
11. Bowen R.M., Compressible porous media models by use of the theory of mixtures, *International Journal of Engineering Science*, **20**, 697–735 (1982)
12. Brooks R.N. and Corey A.T., Properties of porous media affecting fluid flow, *ASCE: Journal of the Irrigation and Draining Division*, **92**, 61–68 (1966)
13. Chen Y., Chen X. and Hisada T., Non-linear finite element analysis of mechanical electrochemical phenomena in hydrated soft tissues based on triphasic theory, *International Journal for Numerical Methods in Engineering*, **65**, 147–173 (2006)
14. Ehlers W., On thermodynamics of elasto-plastic porous media, *Archive of Mechanics*, **41**, 73–93 (1989)
15. Ehlers W., Poröse Medien – ein kontinuumsmechanisches Modell auf der Basis der Mischungstheorie, Habilitation, Forschungsberichte aus dem Fachbereich Bauwesen 47, Universität Essen (1989)
16. Ehlers W., Constitutive equations for granular materials in geomechanical context, In: Continuum Mechanics in Environmental Sciences and Geophysics, (Ed.) Hutter K., CISM Courses and Lectures No. 337, pp. 313–402. Springer, Wien (1993)
17. Ehlers W., A single-surface yield function for geomaterials, *Archive of Applied Mechanics*, **65**, 246–259 (1995)
18. Ehlers W., Grundlegende Konzepte in der Theorie Poröser Medien, *Technische Mechanik*, **16**, 63–76 (1996)
19. Ehlers W., Foundations of multiphasic and porous materials, In: Porous Media – Theory, Experiments and Numerical Applications, (Eds.) Ehlers W. and Bluhm J., pp. 3–86. Springer, Berlin (2002)
20. Ehlers W. and Eipper G., Finite elastic deformations in liquid-saturated and empty porous solids, *Transport in Porous Media*, **34**, 179–191 (1999)
21. Ehlers W., Ellsiepen P., Blome P., Mahnkopf D. and Markert B., Theoretische und numerische Studien zur Lösung von Rand- und Anfangswertproblemen in der Theorie Poröser Medien. Technical Report No. 99-II-1, Institute of Applied Mechanics (CE), Universität Stuttgart (1999)
22. Ehlers W., Ellsiepen P. and Ammann M., Time- and space-adaptive methods applied to localization phenomena in empty and saturated micropolar and standard porous materials, *International Journal for Numerical Methods in Engineering*, **52**, 503–526 (2001)
23. Ehlers W. and Markert B., A linear viscoelastic biphasic model for soft tissues based on the theory of porous media, *ASME Journal of Biomechanical Engineering*, **123**, 418–424 (2001)
24. Ehlers W., Ammann M. and Diebels S., *h*-adaptive FE methods applied to single- and multiphase problems, *International Journal for Numerical Methods in Engineering*, **54**, 219–239 (2002)
25. Ehlers W. and Graf T., On partially saturated soil as a triphasic material, In: Poromechanics II, Proceedings of the 2 nd Biot Conference on Poromechanics, (Eds.) Auriault J.-L., Geindreau C., Royer P., Bloch J.-L., Boutin C. and Lewandowska J., pp. 419–424. Balkema at Swets & Zeitlinger, Lisse (2002)
26. Ehlers W., Markert B. and Acartürk A., Large strain viscoelastic swelling of charged hydrated porous media, In: Poromechanics II, Proceedings of the 2 nd Biot Conference on Poromechanics, (Eds.) Auriault J.-L., Geindreau C., Royer P., Bloch J.-L., Boutin C. and Lewandowska J., pp. 185–191. Balkema at Swets & Zeitlinger, Lisse (2002)
27. Ehlers W., Graf T. and Ammann M., Deformation and localization analysis of partially saturated soil, *Computer Methods in Applied Mechanics and Engineering*, **193**, 2885–2910 (2004)
28. Ehlers W., Markert B. and Acartürk A., Swelling phenomena of hydrated porous materials. In: Poromechanics III, Proceedings of the 3 rd Biot Conference on Poromechanics, (Eds.) Abousleiman Y.N., Cheng A.H.-D. and Ulm F.J., pp. 781–786. Balkema Publishers, Leiden (2005)
29. Ehlers W., Karajan, N. and Markert B., A porous media model describing the inhomogeneous behaviour of the human intervertebral disc, *Materials Science and Engineering Technology*, **37**, 546–551 (2006)
30. Ehlers W. and Scholz B., An inverse algorithm for the identification and the sensitivity analysis of the parameters governing micropolar elasto-plastic granular material, *Archive of Applied Mechanics*, **77**, 911–931 (2007)
31. Ehlers W. and Acartürk A., The role of weakly imposed Dirichlet boundary conditions for numerically stable computations of

swelling phenomena, *Computational Mechanics*, **43**, 545–557 (2009)
32. Ehlers W., Karajan N. and Markert B., An extended biphasic model for charged hydrated tissues with application to the intervertebral disc, *Biomechanics and Modeling in Mechanobiology*, **8**, 233–251 (2009)
33. Ehlers W. and Karajan N., Advances in modelling saturated biological soft tissues and chemically active gels, *Archive of Applied Mechanics*, submitted
34. Eipper G., Theorie und Numerik finiter elastischer Deformationen in fluidgesättigten porösen Medien, Dissertation, Bericht Nr. II-1 aus dem Institut für Mechanik (Bauwesen), Universität Stuttgart (1998)
35. Ellsiepen P., Zeit- und ortsadaptive Verfahren angewandt auf Mehrphasenprobleme poröser Medien, Dissertation, Bericht Nr. II-3 aus dem Institut für Mechanik (Bauwesen), Universität Stuttgart (1999)
36. Finsterle S., Inverse Modellierung zur Bestimmung hydrogeologischer Parameter eines Zweiphasensystems, Dissertation, Technischer Bericht der Versuchsanstalt für Wasserbau, Hydrologie und Graziologie der ETH Zürich (1993)
37. Frijns A.J.H., Huyghe J.M., Kaasschieter E.F. and Wijlaars M.W., Numerical simulation of deformations and electrical potentials in a cartilage substitute, *Biorheology*, **40**, 123–131 (2003)
38. Ghadiani S. R., A multiphasic Continuum-Mechanical Model for Design Investigations of an Effusion-Cooled Rocket Thrust Chamber, Dissertation, Report No. II-13 of the Institute of Applied Mechanics (CE), University of Stuttgart (2005)
39. Graf T., Multiphasic Flow Processes in Deformable Porous Media under Consideration of Fluid Phase Transitions. Dissertation, Report No. II-17 of the Institute of Applied Mechanics (CE), University of Stuttgart (2008)
40. Haupt P., Continuum Mechanics and Theory of Materials, Springer, Berlin (2000)
41. Huyghe J.M. and Janssen J.D., Thermo-chemo-electromechanical formulation of saturated charged porous solids, *Transport in Porous Media*, **34**, 129–141 (1999)
42. Huyghe J.M., Molenaar M.M. and Baaijens F.P.T., Poromechanics of compressible charged porous media using the theory of mixtures, *ASME Journal of Biomechanics*, **129**, 776–785 (2007)
43. Kaasschieter E.F., Frijns A.J.H. and Huyghe J.M.R.J., Mixed finite element modelling of cartilaginous tissues, *Mathematics and Computers in Simulation*, **61**, 549–560 (2003)
44. Karajan N., An Extended Biphasic Description of the Inhomogeneous and Anisotropic Intervertebral Disc. Dissertation, Report No. II-19 of the Institute of Applied Mechanics (CE), University of Stuttgart (2009)
45. Lade P.V. and Duncan J.M., Cubical triaxial tests on cohesionless soil, *ASCE: Journal of Soil Mechanics and Foundations Division*, **99**, 793–812 (1973)
46. Lewis R.W. and Schrefler B.A., The Finite Element Method in the Static and Dynamic Deformation and Consolidation of Porous Media, 2 nd Edition. Wiley, Chichester (1998)
47. Loret B., Hueckel T. and Gajo A., Chemo-mechanical coupling in saturated porous media: elastic-plastic behaviour of homoionic expansive clays, *International Journal of Solids and Structures*, **39**, 2273–2806 (2002)
48. Mahnkopf D., Lokalisierung fluidgesättigter poröser Festkörper bei finiten elastoplastischen Deformationen. Dissertation, Bericht Nr. II-5 aus dem Institut für Mechanik (Bauwesen), Universität Stuttgart (2000)
49. Müllerschön H., Spannungs-Verzerrungsverhalten granularer Materialien am Beispiel von Berliner Sand. Dissertation, Bericht Nr. II-6 aus dem Institut für Mechanik (Bauwesen), Universität Stuttgart (2000)
50. Perzyna P., Fundamental problems in viscoplasticity, *Advances in Applied Mechanics*, **9**, 243–377 (1966)
51. Samson E., Marchand J., Robert J.-L. and Bournazel J.-P., Modelling ion diffusion mechanisms in porous media, *International Journal for Numerical Methods in Engineering*, **46**, 2043–2060 (1999)
52. Scholz B., Application of a Micropolar Model to the Localization Phenomena in Granular Materials: General Model, Sensitivity Analysis and Parameter Optimization. Dissertation, Report No. II-15 of the Institute of Applied Mechanics (CE), University of Stuttgart (2007)
53. Skempton A.W., Significance of Terzaghi's concept of effective stress (Terzaghi's discovery of effective stress), In: From Theory to Practice in Soil Mechanics, (Eds.) Bjerrum L., Casagrande A., Peck R.B. and Skempton A.W., pp. 42–53. Wiley, New York (1960)
54. Truesdell C., Sulle basi delle termomeccanica, *Rendiconti Lincei*, **22**, 158–166 (1957)
55. Truesdell C., Thermodynamics of diffusion, In: Rational Thermodynamics, (Ed.) Truesdell C., 2nd Edition, pp. 219–236. Springer, New York (1984)
56. Truesdell C. and Toupin R.A., The classical field theories, In: Handbuch der Physik, (Ed.) Flügge S., Vol. III/1, pp. 226–902. Springer, Berlin (1960)
57. van Genuchten M.T., A closed-form equation for predicting the hydraulic conductivity of unsaturated soils, *Soil Science Society of America Journal*, **44**, 892–898 (1980)
58. Wallmersperger T., Modellierung und Simulation stimulierbarer polyelektrischer Gele. Dissertation, Institut für Statik und Dynamik der Luft- und Raumfahrtkonstruktionen, Universität Stuttgart (2003)
59. Wieners C., Ammann M., Diebels S. and Ehlers W., Parallel 3-d simulations for porous media models in soil mechanics, *Computational Mechanics*, **29**, 73–87 (2002)
60. Wieners C., Ammann M., Graf T. and Ehlers W., Parallel Krylov methods and the application to 3-d simulations of a triphasic porous media model in soil mechanics, *Computational Mechanics*, **36**, 409–420 (2005)
61. Wieners C., Ammann M. and Ehlers W., Distributed point objects: a new concept for parallel finite elements applied to a geomechanical problem, *Future Generation Computer Systems*, **22**, 532–535 (2006)